

SENSITIVE PARAMETER EVALUATION FOR A VADOSE ZONE FATE
AND TRANSPORT MODEL

Utah State University
Ligan, UT

Jul 89

U.S. DEPARTMENT OF COMMERCE
National Technical Information Service

NTIS[®]

EPA/600/2-89/039
July 1989

SENSITIVE PARAMETER EVALUATION
FOR A VADOSE ZONE FATE AND TRANSPORT MODEL

by

David K. Stevens
William J. Grenney
Zhao Yan
Ronald C. Sims

Department of Civil and Environmental Engineering
Utah State University
Logan, Utah 84322

CR 813211

Project Officer

John E. Matthews
Robert S. Kerr Environmental Research Laboratory
P.O. Box 1198
Ada, Oklahoma 74820

ROBERT S. KERR ENVIRONMENTAL RESEARCH LABORATORY
OFFICE OF RESEARCH AND DEVELOPMENT
U.S. ENVIRONMENTAL PROTECTION AGENCY
ADA, OKLAHOMA 74820

TECHNICAL REPORT DATA
(Please read Instructions on the reverse before completing)

1. REPORT NO. EPA/600/2-89/039		2.		3. RECIPIENT'S ACCESSION NO. PR89 21398749	
4. TITLE AND SUBTITLE SENSITIVE PARAMETER EVALUATION FOR A VADOSE ZONE FATE AND TRANSPORT MODEL				5. REPORT DATE July 1989	
				6. PERFORMING ORGANIZATION CODE	
7. AUTHOR(S) David K. Stevens, William J. Grenney, Zhao Yan, and Ronald C. Sims				8. PERFORMING ORGANIZATION REPORT NO.	
9. PERFORMING ORGANIZATION NAME AND ADDRESS Department of Civil and Environmental Engineering Utah State University Logan, Utah 84322				10. PROGRAM ELEMENT NO. CBWD1A	
				11. CONTRACT/GRANT NO. CR-813211	
12. SPONSORING AGENCY NAME AND ADDRESS Robert S. Kerr Environmental Research Lab. - Ada, OK U.S. Environmental Protection Agency P. O. Box 1198 Ada, OK 74820				13. TYPE OF REPORT AND PERIOD COVERED Final Report (05/86-09/88)	
				14. SPONSORING AGENCY CODE EPA/600/15	
15. SUPPLEMENTARY NOTES Project Officer: John E. Matthews FTS: 743-2233					
16. ABSTRACT This report presents information pertaining to quantitative evaluation of the potential impact of selected parameters on output of vadose zone transport and fate models used to describe the behavior of hazardous chemicals in soil. The Vadose Zone Interactive Processes (VIP) model was selected as the test model for this study. Laboratory and field experiments were conducted to evaluate the effect of sensitive soil and model parameters on the degradation and soil partitioning of hazardous chemicals. Laboratory experiments were conducted to determine the effect of temperature, soil moisture and soil type on the degradation rate. Field-scale experiments were conducted to evaluate oxygen dynamics, through depth and time, for petroleum waste applied to soil. Results of laboratory experiments demonstrated that the sensitivity of the degradation rate to changes in temperature and soil moisture was generally greater for low molecular weight compounds and less for high molecular weight compounds. For the two soil types evaluated, soil type was more significant with regard to immobilization. Soil type was not found to have an effect on degradation kinetics for the majority of chemicals evaluated. The effect of oxygen concentration on chemical degradation as predicted by the test model was found to depend upon the magnitude of the oxygen half-saturation constant. Oxygen-limited degradation would be anticipated to occur shortly after the addition of chemicals to soil and during active microbial metabolism of chemicals.					
17. KEY WORDS AND DOCUMENT ANALYSIS					
a. DESCRIPTORS		b. IDENTIFIERS/OPEN ENDED TERMS		c. COSATI Field, Group	
18. DISTRIBUTION STATEMENT RELEASE TO THE PUBLIC.		19. SECURITY CLASS (This Report) UNCLASSIFIED		21. NO. OF PAGES 94	
		20. SECURITY CLASS (This page) UNCLASSIFIED		22. PRICE	

NOTICE

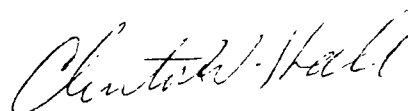
The information in this document has been funded wholly or in part by the United State Environmental Protection Agency under Cooperative Agreement CR-813211 to Utah State University. It has been subjected to the Agency's peer and administrative review, and it has been approved for publication as an EPA document. Mention of trade names or commercial products does not constitute endorsement or recommendation for use.

FOREWORD

EPA is charged by Congress to protect the Nation's land, air and water systems. Under a mandate of national environmental laws focused on air and water quality, solid waste management and the control of toxic substances, pesticides, noise and radiation, the Agency strives to formulate and implement actions which lead to a compatible balance between human activities and the ability of natural systems to support and nurture life.

The Robert S. Kerr Environmental Research Laboratory is the Agency's center of expertise for investigation of the soil and subsurface environment. Personnel at the Laboratory are responsible for management of research programs to: (a) determine the fate, transport and transformation rates of pollutants in the soil, the unsaturated and the saturated zones of the subsurface environment; (b) define the processes to be used in characterizing the soil and subsurface environment as a receptor of pollutants; (c) develop techniques for predicting the effect of pollutants on ground water, soil, and indigenous organisms; and (d) define and demonstrate the applicability and limitations of using natural processes, indigenous to the soil and subsurface environment, for the protection of this resource.

This report presents information pertaining to quantitative evaluation of the potential impact of selected input parameters on output of vadose zone transport and fate models that are used to describe the behavior of hazardous organic chemicals in soil. This evaluation should allow model users to identify those site and model input parameters that have the greatest potential for impacting model output.



Clinton W. Hall
Director
Robert S. Kerr Environmental
Research Laboratory

ABSTRACT

This report presents information pertaining to the development and quantitative evaluation of the mathematical modeling of hazardous chemicals in soil. The Vadose Zone Interactive Processes (VIP) model, based upon the Regulatory and Investigative Treatment Zone (RITZ) model developed at the Robert S. Kerr Environmental Research Laboratory, was evaluated and modified with regard to site-specific dynamic processes. The VIP model was modified to simulate the oxygen transport mechanism in the unsaturated zone, including oxygen transport in air, water, and free hydrocarbon phases with exchange between each phase and losses due to biodegradation. Oxygen-limited degradation was added to the model using a kinetic form that is first order with respect to the organic constituent concentration and mixed order with respect to oxygen concentration. Model output was evaluated as a function of soil oxygen tension, and soil temperature.

Laboratory and field experiments were conducted to evaluate the effect of sensitive soil and model parameters on the degradation and soil partitioning of hazardous chemicals. Laboratory experiments were conducted to determine the effect of temperature, soil moisture, and soil type on degradation rate. Field-scale experiments were conducted to evaluate oxygen dynamics, through depth and time, for petroleum waste applied to soil.

Results of laboratory experiments demonstrated that the sensitivity of degradation rate to changes in temperature and soil moisture was generally greater for low molecular weight compounds and less for high molecular weight compounds. For the two soil types evaluated, soil type was more significant with regard to immobilization; soil type was not found to have an effect on degradation kinetics for the majority of chemicals evaluated.

The effect of oxygen concentration on chemical degradation predicted by the VIP model was found to depend upon the magnitude of the oxygen half-saturation constant. Oxygen-limited degradation would be anticipated to occur shortly after the addition of chemicals to soil and during active microbial metabolism of chemicals.

Model output results for temperature dependent reactions indicated that depth-concentration profiles would be sensitive to and directly related to the temperature correction coefficient (θ) for each chemical. Model outputs would be very sensitive to soil temperature when values for θ was 1.04 or greater.

For the range of values considered for the mass transfer rate coefficient, the VIP model was found to accurately represent nonequilibrium sorption/desorption kinetics enhancement.

Results of laboratory and short-term field studies indicated that site-specific sensitive parameters need to be addressed in modeling the fate and behavior of hazardous chemicals in the unsaturated zone of a soil system. Site-specific sensitive parameters, including soil oxygen concentration and temperature were incorporated into the VIP model in order to evaluate the influence of these parameters on fate and transport. These parameters are

important input for other mathematical models used to describe fate and transport in the vadose zone.

This report was submitted in fulfillment of Cooperative Agreement number 813211 by Utah State University under the sponsorship of the U.S. Environmental Protection Agency. This report covers a period from October 1, 1986 to September 30, 1988, and work was completed as of June 1, 1988.

.

CONTENTS

Notice	ii
Foreword	iii
Abstract	iv
Figures	vii
Tables	ix
Acknowledgments	x
1. Introduction	1
Objectives	2
Approach	2
2. Conclusions	4
3. Recommendations	5
4. Soil Treatment Model	6
Sorption/desorption Kinetics	6
Model Processes	11
Model Equations	16
Model Boundary Conditions	18
Solution Algorithms	19
5. Sensitive Model and Soil Parameters	23
Temperature	23
Oxygen	23
Moisture	24
Soil Type	25
6. Results and Discussion	28
Sensitive Parameters	28
Model Output as a Function of Temperature- dependent Degradation	36
Model Output as a Function of Oxygen- limited Degradation	41
Field Evaluation of Model for Prediction of Oxygen Dynamics	46
Analytical Solution to Two-Phase Model	49
Effect of Mass Transport Coefficient on Model Behavior	61
References	66
Appendix A Nonlinear Least Squares Analysis of Temperature Data	74

FIGURES

<u>Number</u>	<u>Page</u>
1. Schematic diagram of unsaturated aggregated porous medium	8
2. Apparent loss of acenaphthene	29
3. Apparent loss of fluorene	29
4. Apparent loss of phenanthrene	29
5. Apparent loss of anthracene	29
6. Apparent loss of fluoranthene	30
7. Apparent loss of pyrene	30
8. Apparent loss of benz[a]anthracene	30
9. Apparent loss of chrysene	30
10. Apparent loss of benzo[a]pyrene	31
11. Apparent loss of benzo[b]fluoranthene	31
12. Apparent loss of benzo[k]fluoranthene	31
13. Apparent loss of dibenz[a,h]anthracene	31
14. Benzo[g,h,i]perylene degradation	32
15. Indeno[123-c,d]pyrene degradation	32
16. Concentration histories and the predicted first order models for chrysene, benzo[b]fluoranthene, and fluorene	39
17. Depth profiles of chrysene at three different temperatures after one year	42
18. Depth profiles of benzo[b]fluoranthene at three different temperatures after one year	42
19. Depth profiles of fluorene at three different temperatures after one year	42
20. Comparison of the depth profiles with and without oxygen-limits . .	44
21. Constituent and oxygen profiles after 80 days	44

22. Constituent and oxygen breakthrough curves predicted by VIP model	45
23. Depth profiles with five of half oxygen saturation constant coefficients	45
24. Oxygen simulation at depth 6"	48
25. Oxygen simulation at depth 12"	48
26. Oxygen simulation at depth 24"	48
27. Comparison of the depth profiles calculated by the analytical solution to the numerical solution (VIP model) with constituent initially in the water phase	57
28. Comparison of the depth profiles calculated by the analytical solution to the numerical solution (VIP model) with constituent initially in the soil phase	58
29. Comparison of the depth profiles calculated by the analytical solution to the numerical solution (VIP model) with constituent initially in both phases	59
30. Relative error % vs κ in the water phase	60
31. Relative error % vs κ in the soil phase	60
32. Breakthrough curve predicted by VIP model with the initial concentration in the water phase	64
33. Breakthrough curve predicted by VIP model with the initial concentration in the soil phase	64
34. Breakthrough curve predicted by VIP model with the initial concentration in both phases	64

TABLES

<u>Number</u>	<u>Page</u>
1. VIP model boundary conditions	19
2. Percentages of PAH remaining at the end of the 240 day study period and estimated apparent loss half lives	33
3. Arrhenius parameters for the apparent loss of PAH compounds in sandy loam soil	34
4. The effect of soil moisture on degradation rate of PAH compounds in sandy loam soil	34
5. Degradation rates corrected for volatilization for PAH compounds and pesticides applied to two soils	35
6. Calculated soil/water (K_d), partition coefficients for chemicals in two soils	37
7. Estimated values of K_{20} and θ	38
8. Partition coefficients and initial concentrations used in the study	40
9. Degradation summary from VIP Simulation	40
10. Estimates of physical and kinetic parameters	43
11. Input data file for simulation of field data from Nanticoke Refinery	47
12. Model input values for the first two sets of analyses	54
13. Model input values for the last set of analyses	55
14. Descriptions of variables used, units, and data sources	56
15. The definition of the percent relative error and notation	61

ACKNOWLEDGEMENTS

This study was completed for the U.S. Environmental Protection Agency, R.S. Kerr Environmental Research Laboratory. Mr. John Matthews was the project officer.

We wish to acknowledge the support of the U.S. EPA in this endeavor, and, in particular, the candid discussions with Mr. Joe Williams of the EPA on the role and the future of Fate and Transport Modeling in environmental protection.

The participation of Dr. Ryan Dupont of the Department of Civil and Environmental Engineering, Utah State University, in the Nanticoke Refinery field study to generate data used in this report for model evaluation is greatly appreciated.

We would also like to thank Dr. Russell Thompson, Department of Mathematics and Statistics, Utah State University for providing the analytical solutions.

SECTION 1

INTRODUCTION

A mathematical description of the soil/waste system provides a unifying framework for the evaluation of laboratory screening and field data that is useful for the determination of soil treatment potential for a waste. Mathematical models provide an approach for integration of the simultaneous processes of degradation and partitioning in soil systems so that an assessment can be made of the presence of hazardous substances in leachate, soil and air. Models provide an estimate of the potential for groundwater and air contamination through a determination of the rate and extent of contaminant transport and degradation for particular site/soil/compound characteristics. Description of quantitative fate and transport of chemicals in soil systems also allows the identification of chemicals that require management through control of mass transport and/or treatment to reduce or eliminate their hazardous potential (U.S. EPA 1984, Mahmood and Sims, 1986).

Specifically, mathematical models provide a framework for:

- (1) evaluation of literature and/or experimental data;
- (2) evaluation of the effects of site characteristics on soil treatment (soil type, soil horizons, soil permeability);
- (3) determination of the effects of waste concentration, soil moisture, and amendments to increase the rate and/or extent of treatment;
- (4) evaluation of the effects of environmental parameters (season, precipitation) on soil treatment; and
- (5) comparison of the effectiveness of treatment using different practices in order to maximize soil treatment.

Thus mathematical models represent powerful tools for ranking design, operation, and management alternatives as well as for the design of monitoring programs for soil treatment systems.

Short (1986) developed the Regulatory and Investigative Treatment Zone (RITZ) model for evaluating volatilization-corrected degradation and partitioning of organic constituents in soil systems. The RITZ model is generally based on the approach used by Jury et al. (1983) for modeling fate and transport of pesticide in the soil. The RITZ model, developed at the Robert S. Kerr Environmental Research Laboratory (RSKERL), Ada, Oklahoma (U.S. EPA, 1988b), incorporates factors involved in soil treatment at a land treatment facility, including site, soil, and waste characteristics.

The Vadose Zone Interactive Processes (VIP) model, was developed at Utah State University (Grenney et al., 1987), as an enhancement of the RITZ model. The VIP model allows prediction of the behavior of hazardous substances in unsaturated soil systems under conditions of variable precipitation, temperature,

and waste application, and incorporates the effect of oxygen tension on degradation rate in subsurface vadose zone environments. The model simulates vadose zone processes including volatilization, degradation, sorption/desorption, advection, and dispersion (Grenney et al., 1987). The VIP model has been used for predicting the persistence and mobility of petroleum-refining wastes applied to soil treatment systems (Symons et al., 1988), and for the evaluation of the mobility of pesticides in soil (McLean et al., 1988).

Rational mathematical models of soil treatment are based upon conceptual models of soil treatment processes. The degradation process represents an important destructive mechanism for organic substances in soil systems. Important sensitive variables that affect the degradation of organic chemicals in soil include temperature, oxygen concentration, moisture, and soil type (U.S. EPA, 1984 a and b). Therefore, these variables are anticipated to influence the degradation rate of a hazardous substance, which is used as an input variable to these models. These studies incorporated quantitative relationships for temperature and oxygen concentration into the VIP model for the purpose of determining the effects of sensitive parameters on model predictions of chemical fate and transport.

OBJECTIVES

The primary objective of this research project was to experimentally determine the effect of sensitive model and soil parameters on soil treatment and on outputs from vadose zone transport and fate models.

Specific objectives of this research project were to:

- (1) Modify the selected test model (VIP) to simulate the oxygen transport mechanism in the unsaturated zone, including transport in air, water, and free hydrocarbon phases with exchange between each phase and losses due to biodegradation.
- (2) Evaluate model output as a function of soil oxygen concentration.
- (3) Evaluate model output as a function of soil temperature.
- (4) Determine the effects of temperature, oxygen, soil moisture, and soil type on the rate of degradation of organic substances.
- (5) Compare model simulations with field subsurface oxygen measurements.

APPROACH

The test model was evaluated with respect to incorporation of oxygen transport and oxygen-limited biodegradation, and with respect to the effect of temperature on degradation rate. Oxygen-limited biodegradation was added to the VIP model using a kinetic form that is first order with respect to the organic constituent concentration and mixed order (saturation kinetics) with respect to oxygen concentration. A form of the Arrhenius expression was used in the model for the purpose of evaluating the effect of temperature. The method of non-

linear least squares was used to establish the degradation rate at 20°C and the temperature correction coefficient values (θ) for a subset of hazardous substances. Model outputs were evaluated for sensitivity with respect to oxygen concentration and soil temperature. A series of simulations was conducted to evaluate the effects of soil oxygen and temperature on model predictions. The model also was evaluated with respect to nonequilibrium adsorption/desorption in order to more accurately simulate the process of immobilization in a soil system.

A series of laboratory and field experiments were conducted to evaluate the effect of sensitive soil and model parameters on the degradation of hazardous substances. Laboratory experiments were conducted to determine the effect of temperature, soil moisture, and soil type on degradation rate. A field-scale experiment was conducted to evaluate oxygen dynamics, through depth, for a petroleum waste applied to the top six inches of soil.

The test model was evaluated in laboratory column studies using a subset of hazardous substances. Concentration profiles were predicted through depth and through time under unsaturated conditions.

SECTION 2

CONCLUSIONS

Specific conclusions based on the objectives of this research project are:

- (1) Under field conditions with petroleum waste addition, the test model successfully predicted the depth location of the decrease in the oxygen concentration in the air phase, and semi-quantitatively predicted the oxygen concentration. The model did not predict the recovery of oxygen with depth.
- (2) The effect of oxygen concentration on chemical degradation predicted by the test model was found to depend upon the magnitude of the oxygen half-saturation constant and the soil oxygen concentration. Low oxygen concentrations in the soil would be expected to occur shortly after waste addition to soil and during active microbial metabolism of waste.
- (3) Model output results for temperature dependent reactions indicated that depth-concentration profiles were sensitive to and were directly related to the temperature correction coefficient (θ) for each chemical used in the model. Model outputs were very sensitive to soil temperature when values for θ were 1.04 or greater; however, for chemicals with values for $\theta=1.02$ or less, there was little sensitivity in the model output with respect to temperature.
- (4) Results of laboratory experiments demonstrated that the sensitivity of degradation rate to changes in temperature, soil moisture, and soil type was generally greater for low molecular weight compounds and less for high molecular weight compounds.
- (5) The mass transfer rate coefficient, κ , was found to control the extent of dispersion in the absence of an explicit hydrodynamic dispersion term in the transport model.

SECTION 3

RECOMMENDATIONS

Based on the results of this research investigation, the following recommendations are made pertaining to modeling the vadose zone and to evaluating sensitive soil and model parameters:

(1) An intensive, long-term, field-scale evaluation of fate and transport model is recommended for hazardous substances present in a complex waste with respect to air, soil, and leachate phases that builds upon accomplishment of the objectives of this research project.

(2) Further evaluation of degradation kinetic forms as influenced by oxygen concentration is recommended. The kinetic form for oxygen-limited biodegradation provided by Borden and Bedient (1986) increases data requirements for the model, and the trade-off between increased complexity and model accuracy requires further analysis.

(3) A larger subset of hazardous substances is recommended for evaluation of sensitive soil and model parameters that serve as model inputs. While the incorporation of quantitative relationships for oxygen concentration and temperature into the test model was possible, further evaluation is required for development of quantitative relationships for soil moisture and soil type that can be incorporated into mathematical models of the vadose zone.

SECTION 4

SOIL TREATMENT MODEL

Models used to simulate solute transport through soil may be classified into two groups. The first group of models are diffusion-controlled sorption models or two-region models. The liquid phase of the soil is divided into mobile and immobile regions. Convective-diffusive transport is confined to a mobile water phase, while the transfer of solutes into and out of the immobile soil-water region is assumed to be diffusion controlled. The second group of models are two-site kinetic (chemical) adsorption models. The governing nonequilibrium adsorption/desorption system equations use first-order mass transfer kinetics in considering a two-phase (water and soil environment) chemical process.

$$\frac{\partial C}{\partial t} + (\rho/\theta) \frac{\partial S}{\partial t} = -V_w \frac{\partial C}{\partial x} + D_a \frac{\partial^2 C}{\partial x^2} \quad [1a]$$

$$\frac{\partial S}{\partial t} = \kappa K (K_{sw} C - S) \quad [1b]$$

where:

- C is the concentration of the chemical in solution (g/m³),
- S is the amount of chemical adsorbed per gram of soil (g/g),
- V_w is the vertical pore-water velocity (m/day),
- ρ is bulk density of the soil (g/m³),
- θ is the water content (m³/m³),
- x is the depth, positive downward (m),
- t is time (days),
- D_a is the dispersion coefficient (m²/day),
- K_{sw} is the partition coefficient for soil with respect to the water phase (g/g-soil)/(g/m³-water), and
- κ (kappa) is the mass transfer rate coefficient (day⁻¹), a parameter for describing the exchange rate between the water phase and soil phase.

SORPTION/DESORPTION KINETICS

Lapidus and Amundson (1952) first developed a parabolic partial differential equation model to describe mass transport of chemicals in porous media. Hashimoto et al. (1964) discussed these equations and Kay and Elrick (1967) used these equations to describe the movement of lindane through soils. Lindstrom and Boersma (1971) obtained the solutions of the resulting initial value problem with conservation type boundary conditions for the case of water saturated, sorbing porous medium. In a later paper, Lindstrom et al. (1971) suggested a more comprehensive model of sorption, and solved it numerically, involving the relationship between the free and sorbed phases of the medium.

In addition, Lindstrom and Narasinhham (1973) obtained an exact solution to the problem for the first order kinetics of sorption which requires a large activation energy.

Two-region Model

More recent attempts to model the solute transport through soil may be classified into two groups. The first group of models are diffusion-controlled sorption (physical) models or two region models. The liquid phase of the soil is divided into mobile and immobile regions. Convective-diffusive transport is confined to only a fraction of the liquid-filled pores (mobile water phase), while the remainder of the pores contain stagnant water. This stagnant water has been visualized as thin liquid films around soil particles, dead-end pores (Coats and Smith, 1964), non-moving intra-aggregate water (Philip, 1968; Passioura, 1971), or as relatively isolated regions associated with unsaturated flow (Neilsen and Biggar, 1961). The transfer of solutes into and out of the immobile soil-water region is assumed to be diffusion controlled. Transport models based on first-order exchange rates of solute between mobile and stagnant regions were initially discussed in the petroleum and chemical engineering literature for nonsorbing chemicals (Coats and Smith, 1964). van Genuchten and Wierenga (1976) presented a schematic diagram to describe the movement of a chemical through an unsaturated, aggregated sorbing porous medium. Five different regions can be identified (see Figure 1).

- 1) Air spaces.
- 2) Mobile (or dynamic) water, located inside the larger (inter-aggregate) pores. The flow of fluid in the medium is assumed to occur in this region only. Solute transfer occurs by both convection and longitudinal diffusion.
- 3) Immobile (dead or stagnant) water, located inside aggregates and at the contact points of aggregates and/or particles. In saturated media this region is mainly confined to intra-aggregate pores. Note that air-bubbles and unsaturated conditions may increase the proportion of dead water by creating more dead-end pores.
- 4) A dynamic soil region, located sufficiently close to the mobile water phase for equilibrium (assumed) between the solute in the mobile liquid.
- 5) A stagnant soil region, that part of the soil matrix where sorption is diffusion limited. This part of the soil is located mainly around the micro-pores inside the aggregates, or along dead-end water pockets. Sorption occurs here only after the chemical has diffused through the liquid barrier of the immobile liquid phase.

Van Genuchten and Wierenga (1976) extended the above concepts of mobile-immobile water to include Freundlich-type equilibrium sorption-desorption processes. Their equations are of the form

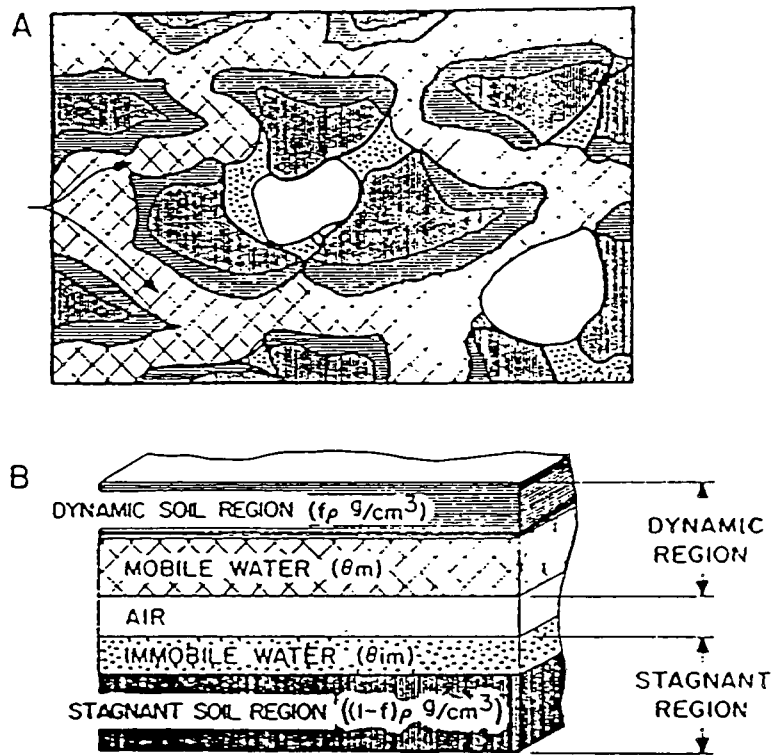


Figure 1. Schematic diagram of unsaturated aggregated porous medium
 (A) Actual model. (B) Simplified model.

$$\theta_m R_m \frac{\partial c_m}{\partial t} + \theta_{im} R_{im} \frac{dc_{im}}{dt} = \theta_m D_m \frac{\partial^2 c_m}{\partial x^2} - \theta_m v_m \frac{\partial c_m}{\partial x} \quad [2a]$$

$$\theta_{im} R_{im} \frac{dc_{im}}{dt} = \alpha (c_m - c_{im}) \quad [2b]$$

where:

c_m and c_{im} are the concentrations (g/m³) in both the mobile and stagnant regions,

θ_m and θ_{im} are the fractions of the soil filled with mobile and stagnant water (m³/m³), respectively,

v_m is the average pore-water velocity in the mobile liquid,

α is a mass transfer coefficient (day⁻¹),

R_m and R_{im} are retardation factors to account for equilibrium type sorption processes in the mobile and immobile regions, respectively,

D_m is the dispersion coefficient in the mobile liquid.

The mass transfer coefficient α is interpreted as a diffusion coefficient divided by some average diffusional path length (Nielsen, 1986). Valocchi (1985), Nkedi-Kizza et al. (1984), Rao and Jessup (1983), van Genuchten and Cleary (1979), Rao et al. (1980a,b), van Genuchten and Wierenga (1976), and van Genuchten et al. (1984) present more discussion on this type of model.

Two-site Model

The second group of conceptual models are two-site kinetic (chemical) sorption models. Selim et al. (1976), and Cameron and Klute (1977) have independently proposed this type of model to describe solute sorption on heterogeneous solid surfaces. Rao et al. (1979) used this type of model for pesticide sorption, while Hoffman and Rolston (1980) and De Camargo et al. (1979), used this model for phosphorus sorption. Additional application can be found in the work of Nielsen et al. (1986) and Nkedi-Kizza et al. (1984). In this model, two types of sorption sites are hypothesized: type 1 reaches equilibrium instantaneously and type 2 are time-dependent kinetic sorption models. The diffusion-controlled process (model 2) is not explicitly analyzed in this work, however, Nkedi-Kizza et al. (1984) have shown that the diffusion-controlled model is mathematically equivalent to a first order kinetic model.

The governing solute transport equations for a two-site chemical process sorptive model are as follows:

$$\frac{\partial C}{\partial t} + (\rho/\theta) \frac{\partial S}{\partial t} = -V_w \frac{\partial C}{\partial x} + D_a \frac{\partial^2 C}{\partial x^2} \quad [3a]$$

$$\frac{\partial S}{\partial t} = f(C, S) \quad [3b]$$

where:

C is the concentration of the chemical in solution (g/m³),
 S is the amount of chemical sorbed per gram of soil (g/g),
 V_w is the vertical pore-water velocity (m/day),
 ρ is bulk density of the soil (g/m³),
 θ is the water content (m³/m³),
 x is the depth, positive downward (m),
 t is time (days),
 D_a is the dispersion coefficient (m²/day),

Several conceptual models have been proposed and evaluated for describing the solute sorption-desorption term (∂S/∂t) in Eq. [3b]. Three of the most common special cases were discussed by van Genuchten (1974):

1) Freundlich equation

$$S = KC^N \quad [4]$$

Differentiation of Eq [4] with respect to time gives:

$$\frac{\partial S}{\partial t} = KNC^{N-1} \frac{\partial C}{\partial t} \quad [5]$$

2) The first order kinetic rate equation

$$\frac{\partial S}{\partial t} = \kappa(K_{sw}C - S) \quad [6]$$

3) Exponential equation

$$\frac{\partial S}{\partial t} = k_2 e^{bS} \left(\frac{k_1 e^{-2bS} \theta}{k_2 \rho} C - S \right) \quad [7]$$

where

k₁ is the forward kinetic rate coefficient (1/day),
 k₂ is the backward kinetic rate coefficient (1/day),
 b is similar to the surface stress coefficient (g/μg), described by Fava and Eyring (1956). For equilibrium sorption (∂S/∂t = 0), Eq. [7] reduces to

$$S = \frac{\theta k_1 C}{\rho k_2} e^{-2bS} \quad [8]$$

Most previous work considered the equilibrium (type 1) model and to a lesser extent utilized the nonequilibrium model. Lindstrom et al. (1971) and Lindstrom and Narasinhham (1973) considered nonequilibrium conditions and discussed the mass transfer coefficient. In this report, we adopt the first order kinetic model as the topic under discussion.

Mass Transfer Rate Coefficient

Rao et al. (1980a; 1980b) presented a theoretical and experimental analysis of the mass transfer rate coefficient (α) for a two-region (physical nonequilibrium) model and indicated that the mass transfer coefficient (α) for the two-region model is dependent upon the soil particle sphere radius, time of diffusion, volumetric water contents inside and outside the sphere, and the molecular diffusion coefficient. However, relatively little is known concerning the factors that affect the mass transfer rate coefficient (κ) in two-site (chemical nonequilibrium) models.

MODEL PROCESSES

The VIP model as presented in this report extends previous work by Short (1986) and Grenney, et al. (1987) for use in screening specific hazardous wastes from land treatment. The model describes a soil column 1.0 meter square with depth specified by the user. A constituent, which refers to the hazardous substance being tracked by the model, may be a pure compound or a mixture of several compounds as long as the behavior of the mixture can be adequately described by composite constituent parameters.

The model was developed under the following assumptions:

- 1) One dimensional soil system is assumed.
- 2) The soil column consists two isothermal layers: a plow zone (Zone of Incorporation, ZOI) and a lower treatment zone (LTZ). The plow zone is typically defined as the top 15 cm of soil into which the substance is mixed during application. The LTZ extends below the ZOI to the bottom of the soil column and contains substances which have been mobilized and transported downward from the ZOI.
- 3) Unsaturated flow is assumed. The pore velocity of the water phase is calculated by dividing the average infiltration rate (V_w') by the water content of the soil (θ_w). The water content is estimated from the soil properties and water net infiltration rate by the procedure of Clapp and Hornberger (1978):

$$\theta_w = \phi \left[\frac{V'}{c} \right]^{1/(2b+3)} \quad [9]$$

where:

- V' = recharge rate (cm/day)
- c = saturated hydraulic conductivity (cm/day)
- b = coefficient dependent on soil properties.

- 4) The soil environment within the column is made up of four phases: soil grains, pore water, pore air, and pore oil.
- 5) First order non-equilibrium kinetics describes partitioning of the chemical constituent between the water, soil, oil and air phases, and partitioning of oxygen between the water, oil and air phases.
- 6) Degradation of oil and constituents in water, soil, air and soil phases are expressed as a combination of the first order decay and a modified Monod function for oxygen limitation.
- 7) Characteristics of the soil environment (site recharge rate, site temperature and saturated hydraulic conductivity) can be changed with depth and/or time.
- 8) Waste material is applied to the plow zone at loading rates and frequencies specified by the user. It is completely mixed in the plow zone.
- 9) The oil in the waste does not migrate. Only the chemical constituents move with the soil water.
- 10) Longitudinal dispersion is insignificant in the water phase and neglected, but included in oxygen and the air phase. Plug flow of water in plow zone and treatment zone is assumed.

In this model, hydrodynamic dispersion is assumed to be negligible. This assumption is based on the notion that, under unsaturated flow conditions, flow velocities and turbulence levels are very small, fractions of those encountered in saturated porous media. The causes of hydrodynamic dispersion are many but the effects are primarily influenced by fluid turbulence, large density and velocity gradients, and anisotropy of the fluid flow regime. Under prevailing conditions in the vadose zone, these forces do not control the flow regime.

This phenomenon was evaluated by Mears (1971), who suggested a criterion for trickle-flow reactors at low Reynolds number with first order kinetics, whereby for dispersion to be safely neglected,

$$\frac{Z}{d_p} > \frac{20}{B_o} \ln(C_o/C_f)$$

where Z is the depth of the soil, d_p is particle diameter, C_o is the influent concentration, C_f is the effluent concentration, and B_o is Bodenstein number, which is equal to Vd_p/D_1 (D_1 is the hydrodynamic dispersion coefficient and V is the fluid velocity), Petersen (1963) summarized considerable work that suggested that $B_o \approx 0.5$ for low Reynolds numbers when the hydrodynamic regions are interlocking. By this criterion using $C_o/C_f=100$ (99% reduction of the constituent), for hydrodynamic dispersion to be important, $Z/d_p=184.2$. For typical soils with $d_p \approx 0.02$ cm, $Z > 3.7$ cm for axial dispersion to be neglected. Thus, axial dispersion will only be important for very short columns of little practical interest. Further, the dispersion process necessarily relies on a continuum of fluid pathways. In the vadose zone, those pathways are not continuous - the area of contact through which the flux may occur is a small fraction of that which exists under saturated flow. Thus, the fluid attributes necessary for the process to occur are missing. For these reasons, hydrodynamic dispersion is neglected.

The model simulates the fate of hazardous organic substances in the soil. The fate of a constituent in the soil column depends on mobilization, volatilization, and decomposition processes. The model also simulates oxygen transport in the unsaturated zone which includes transport by air, water, and free hydrocarbon phases with exchange between each phase and losses due to biodegradation of the hazardous waste constituents within the soil column. Equation [9] describes these processes mathematically for one phase in a control volume slice (thickness = dz) of a one-dimensional (vertical) soil column.

$$\frac{\partial(C\theta A)}{\partial t} dz = \frac{\partial(\theta AD(\partial C/\partial z))}{\partial z} dz + \frac{\partial(-V\theta AC)}{\partial z} dz + \psi A dz - RC\theta A dz \quad [10]$$

where:

- A = horizontal area of the control volume, (m^2)
- C = concentration of the constituent or oxygen in the phase (g/m^3)
- D = dispersion coefficient for the phase, (m^2/day)
- dz = depth of control volume, (m)
- t = time, ($days$)
- V = vertical pore velocity of the phase, (m/day)
- z = depth, positive downwards (m)
- θ = volume of the phase within the control volume, (m^3 phase/ m^3 control volume)
- ρ = bulk density of the soil ($g\text{-soil}/m^3$ control volume)
- R = degradation rate for the constituent or oxygen within the phase, ($1/day$)
- ψ = mass sorption rate into the phase from other phases, ($g/day/m^3$ control volume)

Mobilization (transport)

Once applied to the land and mixed into the plow zone, a constituent may be mobilized by three mechanisms: advection, dispersion, and migration between/among phases. Oxygen transport in a soil column may also include these three mechanisms.

Dispersion. Mobilization by dispersion of the phase within the soil column is represented by the first term on the right-hand-side of Equation [9]. Dispersion is simulated for chemical constituents in the air phase. Dispersion in the water phase has been inactivated in this version of the model because the nonequilibrium sorption/desorption process (described later) provided dispersive phenomena sufficient to simulate observed behavior. However, if and when activated, it will be solved by a scheme similar to that for air. The oxygen dispersion mechanism is assumed significant only in the air phase using the air dispersion coefficient (D_a).

Advection. The advection mechanism is represented by the second term on the right-hand-side of Equation [10]. It may be significant for the water and air phases. Oxygen transport by advection of the phase within the soil column is assumed significant for the water and air phases with the pore velocity of the water (V_w) and air (V_a) phases. Although in some applications advection may also be significant for the oil phase, this version of the model constrains the oil to the plow zone. Laboratory experiments on mobility of the oil phase in soil are currently underway at Utah State University (USU). The soil grain phase is assumed to be immobile.

Sorption/desorption. The third term on the right-hand-side of Equation [10] represents migration of the constituent or oxygen between/among phases. This mass flux of the constituents or oxygen among phases is modeled as a sorption mechanism. Grenney et. al (1987), Enfield et. al (1986) and Lapidus and Amundson (1952) have expressed the sorption mechanism as a linear gradient process of the following form:

$$\psi = - \kappa (K_{2,1}C_2 - C_1) \quad [11]$$

where:

- ψ = mass flux of oxygen or constituent ($\text{g}/\text{m}^3\text{-day}$)
- C_1 = oxygen or constituent concentration in Phase 1 (g/m^3)
- C_2 = oxygen or constituent concentration in Phase 2 (g/m^3)
- κ = mass transfer rate coefficient (day^{-1})
- $K_{2,1}$ = linear partition coefficient for Phase 2 with respect to Phase 1 ($\text{g}/\text{m}^3\text{-Phase 2})/(\text{g}/\text{m}^3\text{-Phase 1})$

In general sorption can occur directly between any two phases that are in contact, and Equation [11] could be expanded to describe mass flux among more than two phases at a time. However, estimating meaningful values for the additional coefficients would be extremely difficult, and so it is assumed that constituent migration from one phase to another must pass through the water phase. Consequently, Equation [11] is applied between the water phase and each of the other phases (Enfield et. al, 1986, Short, 1986). For the case of oxygen, it is assumed that migration from one phase to another must pass through the air phase, and there is no oxygen sorbed by the soil grain. Consequently, Equation [11] is applied between the air phase and water or oil phases.

Volatilization

Volatilization is represented in the model by two processes: mass flux into the air phase and advection/dispersion. The mass flux of the constituent into the air phase is modeled by a sorption mechanism. The constituent is then transported with the air phase by advection and/or dispersion, depending on the conditions at the soil surface.

Degradation

The fourth term of Equation [10] represents the degradation (biochemical, photochemical or hydrolytic). Field and laboratory studies of other investigators, Sims, et al. (1988) and Sims and Overcash (1983), have indicated that the use of first order kinetics provides a reasonable approximation for the degradation of many hazardous substances in soil systems. Baehr and Corapcioglu (1984) have presented a one-dimensional model for simulating gasoline transport in the unsaturated zone which includes transport by air, water, and free hydrocarbon phases with exchange between each phase and losses due to biodegradation. Borden and Bedient (1986) and Molz et al. (1986) noted that the microbial metabolism can be limited by a lack of either substrate (carbon and energy source), oxygen (electron acceptor) or both simultaneously. The removal of hydrocarbon and oxygen in each phase can be represented by a modified Monod kinetic relationship where:

$$\frac{dC}{dt} = -M_t k \frac{C}{K_c + C} \frac{O}{K_o + O} \quad [12a]$$

$$\frac{dO}{dt} = -M_t k \nu_c \frac{C}{K_c + C} \frac{O}{K_o + O} \quad [12b]$$

where:

- C is the concentration of the hydrocarbon;
- O is the concentration of oxygen;
- M_t is the total microbial concentration;
- k is the maximum hydrocarbon utilization rate per unit mass of microorganisms;
- ν_c is the ratio of oxygen to hydrocarbon consumed;
- K_c is the hydrocarbon half saturation constant;
- K_o is the oxygen half saturation constant;
- t is time.

The degradation expression of the VIP model used in these studies to evaluate sensitive model parameters combines the first order kinetics described by Grenney et al., (1987) with a modified Monod function for oxygen limitation:

$$\frac{dC}{dt} = -\mu C \frac{O}{K_o + O} \quad [13a]$$

$$\frac{dO}{dt} = -v_c \mu C \frac{O}{K_o + O} \quad [13b]$$

where μ is the constituent first order decay rate (day^{-1}).

Because the constituent may degrade at different rates in different phases, separate rate and half-saturation coefficients are provided for each phase in the model. The apparent degradation rate coefficients are permitted to vary with depth in the model.

MODEL EQUATIONS

Based on the preceding discussion, the model equations for the four phases within a soil column of unit cross-sectional area can be expressed as follows:

$$\begin{aligned} \frac{\partial C_w}{\partial t} = & -V_w \frac{\partial C_w}{\partial z} - \mu_w C_w \frac{O_w}{K_w + O_w} \\ & - (\theta_a / \theta_w) \kappa_a (K_{aw} C_w - C_a) \\ & - (\theta_o / \theta_w) \kappa_o (K_{ow} C_w - C_o) \\ & - (\rho / \theta_w) \kappa_s (K_{sw} C_w - C_s) \end{aligned} \quad [14a]$$

$$\begin{aligned} \frac{\partial C_a}{\partial t} = & -V_a \frac{\partial C_a}{\partial z} + D_a \frac{\partial^2 C_a}{\partial z^2} - \mu_a C_a \frac{O_a}{K_a + O_a} \\ & + \kappa_a (K_{aw} C_w - C_a) - \frac{C_a}{\theta_a} \frac{\partial \theta_a}{\partial t} \end{aligned} \quad [14b]$$

$$\frac{\partial C_o}{\partial t} = -\mu_o C_o \frac{O_o}{K_o + O_o} + \kappa_o (K_{ow} C_w - C_o) - \frac{C_o}{\theta_o} \frac{\partial \theta_o}{\partial t} \quad [14c]$$

$$\frac{\partial C_s}{\partial t} = -\mu_s C_s \frac{O_w}{K_w + O_w} + \kappa_s (K_{sw} C_w - C_s) \quad [14d]$$

$$\frac{\partial \theta_o}{\partial t} = - \gamma_o \theta_o \frac{O_o}{K_{oo} + O_o} \quad [14e]$$

$$\theta_a = \phi - \theta_w - \theta_o \quad [14f]$$

$$\frac{\partial O_o}{\partial t} = - \nu_c \mu_o C_o \frac{O_o}{K_o + O_o} + \kappa_o^a (K_{oa} O_a - O_o) -$$

$$(\rho_o \nu_o + O_o) \frac{1}{\theta_o} \frac{\partial \theta_o}{\partial t} \quad [14g]$$

$$\begin{aligned} \frac{\partial O_w}{\partial t} = & - V_w \frac{\partial O_w}{\partial z} - \nu_c \mu_w C_w \frac{O_w}{K_w + O_w} - \nu_c \mu_s C_s \frac{O_w}{K_w + O_w} \\ & + \kappa_w^a (K_{wa} O_a - O_w) \end{aligned} \quad [14h]$$

$$\begin{aligned} \frac{\partial O_a}{\partial t} = & V_a \frac{\partial O_a}{\partial z} + D_a \frac{\partial^2 O_a}{\partial z^2} - \nu_c \mu_a C_a \frac{O_a}{K_a + O_a} \\ & - (\theta_w / \theta_a) \kappa_o^a (K_{wa} O_a - O_w) \\ & - (\theta_o / \theta_a) \kappa_o^o (K_{oa} O_a - O_o) - \frac{O_a}{\theta_a} \frac{\partial \theta_a}{\partial t} \end{aligned} \quad [14i]$$

where:

- C_o = concentration of the constituent in the oil phase (g/m^3)
- C_a = concentration of the constituent in the air phase (g/m^3)
- C_w = concentration of the constituent in the water phase (g/m^3)
- C_s = concentration of the constituent in the soil phase (g/m^3)
- K_{aw} = constituent partition coefficient between air phase and water phase ($\text{g}/\text{m}^3\text{-air}/(\text{g}/\text{m}^3\text{-water})$)
- K_{ow} = constituent partition coefficient between oil phase and water phase ($\text{g}/\text{m}^3\text{-oil}/(\text{g}/\text{m}^3\text{-water})$)
- K_{sw} = constituent partition coefficient between soil phase and water phase ($\text{g}/\text{g-soil}/(\text{g}/\text{m}^3\text{-water})$)
- ϕ = soil porosity (m^3/m^3)
- ρ = soil bulk density (g/cm^3)
- μ_o = constituent degradation rate in the oil phase (day^{-1})
- μ_a = constituent degradation rate in the oil phase (day^{-1})

μ_w	=	constituent degradation rate in the water phase (day^{-1})
μ_s	=	constituent degradation rate in the soil phase (day^{-1})
γ	=	the degradation rate of the oil phase (day^{-1})
O_o	=	oxygen concentration in the oil phase (g/m^3)
O_w	=	oxygen concentration in the water phase (g/m^3)
O_a	=	oxygen concentration in the air phase (g/m^3)
K_o	=	oxygen half saturation constant with respect to the constituent decay in the oil phase (g/m^3),
K_w	=	oxygen half saturation constant with respect to the constituent decay in the oil phase (g/m^3)
K_a	=	oxygen half saturation constant with respect to the constituent decay in the air phase (g/m^3)
K_{oo}	=	oxygen half saturation constant with respect to the oil decay (g/m^3)
K_{oa}	=	oxygen partition coefficient between the oil and air phases ($\text{g-O}_2/\text{m}^3\text{-oil phase}/(\text{g-O}_2/\text{m}^3\text{-air phase})$)
K_{wa}	=	oxygen partition coefficient between the water and air phases ($\text{g-O}_2/\text{m}^3\text{-water phase}/(\text{g-O}_2/\text{m}^3\text{-air phase})$)
κ_a	=	constituent transfer rate coefficient between the water and air phases (day^{-1})
κ_o	=	constituent transfer rate coefficient between the water and oil phases (day^{-1})
κ_s	=	constituent transfer rate coefficient between the water and soil phases (day^{-1})
κ_o^a	=	oxygen transfer rate coefficient between the oil and air phases (day^{-1})
κ_w^a	=	oxygen transfer rate coefficient between the water and air phases (day^{-1})
ν_c	=	stoichiometric ratio of the oxygen to the constituent consumed
ν_o	=	stoichiometric ratio of the oxygen to the oil consumed
θ_a	=	volume of the air phase within the control volume, ($\text{m}^3\text{-air}/\text{m}^3\text{-control volume}$)
θ_w	=	volume of the water phase within the control volume, ($\text{m}^3\text{-water}/\text{m}^3\text{-control volume}$)
θ_o	=	volume of the oil phase within the control volume, ($\text{m}^3\text{-oil}/\text{m}^3\text{-control volume}$)
V_w	=	pore water velocity, (cm/day)
ρ_o	=	density of the oil (g/cc)

MODEL BOUNDARY CONDITIONS

The boundary conditions of the VIP model are constituent and oxygen concentrations at the upper and bottom layers of the soil column, and initial conditions of concentration and water, air, and oil saturation with depth. The model boundary conditions are presented in Table 1.

Table 1. VIP Model Boundary Conditions

Boundary	Phase									
	Air			Water			Soil	Oil		
	C_a	O_a	θ_a	C_w	O_w	θ_w	C_s	C_o	O_o	θ_o
$z = 0$	0	$P_{O_2}^*$	-- ⁺	0	$K_{wa}P_{O_2}$	--	--	--	--	--
$z = Z$	0	P_{O_2}	--	0	$K_{wa}P_{O_2}$	--	--	--	--	--
$t = 0$	C_{ao}	O_{ao}	θ_{ao}	C_{wo}	O_{wo}	θ_{wo}	C_{so}	C_{oo}	O_{oo}	θ_{oo}

* No condition required.

⁺ Partial pressure of oxygen in atmosphere (300 g/m³).

SOLUTION ALGORITHMS

The model Equations [14a] - [14i] are programmed in FORTRAN and solved numerically. The program will run on IBM-PC, -XT, -AT, and PS/2 compatible equipment, and has a built-in editor or accepts input files from LOTUS spreadsheets. An option for graphical output is provided.

The computer code is designed in a modular structure to provide for convenient enhancement in the future. The modular structure also provides a convenient means for evaluating the behavior of various processes by isolating the modules for independent analysis. The main solution algorithm is divided into functional modules: loading rates, degradation, oil decay, and phase transport and sorption.

Loading rates

The user specifies the initial oxygen concentration and initial constituent concentration profile in the soil column and the frequency of waste application. Each waste application is assumed to be instantaneously and uniformly incorporated into the zone of incorporation (ZOI). This is accomplished by establishing a new initial condition to account for the

additional mass in the ZOI each time waste is applied.

Degradation

This module solves the degradation terms of Equations [14a], [14b], [14d], [14h] and [14i] for the oxygen and constituents in air, water and soil phases. The concentration of the oxygen or a constituent remaining in the water, air or soil phases at the end of a finite time interval (Δt) is calculated by:

$$C_{(t+\Delta t)} = C_{(t)} \exp \left[-\mu \Delta t \frac{0}{K_o + 0} \right] \quad [15]$$

The solution for the constituent degradation in the oil phase, oil phase decay, and oxygen consumption is accomplished by expressing the Equation [14c], [14e] and [14g] as implicit difference equations across the time increment (Δt). The resulting equations are then solved simultaneously by the Newton-Raphson method.

Phase transport

The constituent or oxygen is transported by advection of the water phase and by advection and dispersion of the air phase. The advective transport of the water phase is formulated as an explicit, upstream difference (Bella and Grenney, 1970) as follows:

$$C_{(i,t+\Delta t)} = C_{(i,t)} + (C_{(i-1,t)} - C_{(i,t)}) \hat{V} \Delta Z / \Delta t \quad [16]$$

where \hat{V} is an adjusted velocity and Δt is calculated such that:

$$\hat{V} \Delta t / \Delta Z = 1 \quad [17]$$

This formulation provides an exact solution for the advective water transport and will preserve a vertical concentration gradient at the leading edge of the transport wave. The parameter \hat{V} is obtained by adjusting the pore velocity of the water, V_w , to account for the retardation caused by sorption as described later. Experience has been gained over the years concerning the behavior of numerical solutions for the advection and dispersion of water quality constituents. The advection and dispersion terms have been solved successfully for steady and unsteady flow by explicit (Bella, 1970; Holley, 1965; Hann, 1972) and implicit techniques (Hann, 1972; Harleman, 1968; O'Connor, 1968; Prych, 1969; Grenney, 1978).

The dispersion terms of the air phase are formulated as an implicit difference equation:

$$C_{i,t} = A_1 C_{i-1,t+\Delta t} + A_2 C_{i,t+\Delta t} + A_3 C_{i+1,t+\Delta t} \quad [18]$$

$$A_1 = -D_a \Delta t / \Delta z^2$$

$$A_2 = 1 + 2D_a \Delta t / \Delta z^2$$

$$A_3 = -D_a \Delta t / \Delta z^2$$

The system of Equations [18] is expressed in matrix form and solved by numerical techniques.

Sorption/desorption

The method involves solving the kinematic terms in each of the Equations [14a] - [14i]. This is accomplished by expressing them as implicit difference equations across the time increment (Δt). For each control volume (i):

$$\begin{aligned} \frac{C_{w(t+\Delta t)} - C_{w(t)}}{\Delta t} &= -\kappa_o(K_{ow}C_{w(t+\Delta t)}) \frac{\theta_o}{\theta_w} - C_{o(t+\Delta t)} \\ &\quad -\kappa_o(K_{aw}C_{w(t+\Delta t)}) \frac{\theta_a}{\theta_w} - C_{a(t+\Delta t)} \\ &\quad -\kappa_s(K_{sw}C_{w(t+\Delta t)}) \frac{\rho}{\theta_w} - C_{s(t+\Delta t)} \\ \frac{C_{o(t+\Delta t)} - C_{o(t)}}{\Delta t} &= \kappa_o(K_{ow}C_{w(t+\Delta t)} - C_{o(t+\Delta t)}) \end{aligned} \quad [19b]$$

The equations for air and soil are identical in form to Equation [19b] for oil. These equations are rearranged and solved by a one-pass matrix reduction procedure. The system of equations and the numerical method preserve the mass balance across the time increment. Oxygen partitioning is calculated using Equations [19a] and [19b] with the air phase as the common medium.

Modular approach

There are three important benefits to programming numerical techniques in functional modules. First, the program is easy to modify and upgrade. Second, more than one solution procedure can be used, thereby allowing the use of a specific technique (closed-form, explicit, implicit) best suited for the

equations in each module. Third, the behavior of the various physical and biochemical mechanisms being represented may be evaluated by isolating the modules for independent analysis. These features also enhance the use of the model as a research tool because a variety of hypotheses, expressed as mathematical equations, may be conveniently inserted and tested.

SECTION 5

SENSITIVE MODEL AND SOIL PARAMETERS

Important sensitive variables that may impact soil treatment include temperature, soil oxygen, soil moisture, and soil type.

TEMPERATURE

Soil temperature is expected to be one of the most sensitive parameters affecting soil treatment (Smith, 1982) and model output. The effect of temperature on soil degradation reaction rate may follow the Arrhenius relationship which has been used to correlate environmental temperature and reaction rate in soils (Hamaker 1972, Dibble 1979, Lyman et al. 1982, and Parker 1983).

In this research project the effect of temperature on the rate of degradation in a Kidman sandy loam soil was experimentally determined for 16 polynuclear aromatic hydrocarbon (PAH) compounds. Soil properties determined prior to initiation of the study include a soil pH of 7.9, 0.5% by weight organic carbon, 0.06% by weight total phosphorus, 0.07% by weight total nitrogen and a water holding capacity of 16% by weight. These compounds were evaluated because of their presence in petroleum and wood preservative organic wastes and because of their public health implications (Sims and Overcash 1983). A standard solution of 16 PAH compounds in dichloromethane was added to the soil to achieve an equivalent one percent by weight creosote addition to soil. The loading used resulted in the following soil concentrations (mg/kg soil dry-weight): naphthalene (501), acenaphthylene (30.4), acenaphthene (400), fluorene (100), phenanthrene (1000), anthracene (600), fluoranthene (400), pyrene (400), benzo[a]anthracene (30.1), chrysene (200), benzo[b]fluoranthene (9.94), benzo[k]fluoranthene (9.98), benzo[a]pyrene (10.76), dibenz[a,h]anthracene (10.56), benzo[ghi]perylene (9.96), and indeno[1,2,3-cd]pyrene (5.25). Temperatures evaluated were 10°, 20°, and 30°C.

Moisture content of the soil-PAH mixtures in glass beaker microcosms was maintained between 80 and 100% of the soil water holding capacity. Periodically through time triplicate sets of microcosms at each temperature were removed from incubation and solvent extracted with dichloromethane. Concentrations of PAHs in soil were determined by HPLC analysis of the extracts. The study was terminated after 240 days of incubation.

OXYGEN

Microbial respiration removes oxygen from the soil atmosphere and enriches it with carbon dioxide. While gases diffuse freely into and out of the soil environment across the air/soil interface, the oxygen concentration in normal soil air may be only half that of atmospheric levels, while concentrations of carbon dioxide may be many times higher than in the surface air (Brady 1974). A large fraction of the microbial population within the soil environment depends

upon oxygen to serve as its terminal electron acceptor in their metabolism. Bacteria of the genus Pseudomonas, members of which are often linked to the soil transformation of xenobiotic compounds, are strict aerobes. Under oxygen-restricted conditions, facultative organisms, those which use alternative electron acceptors such as nitrate (denitrifiers) or sulfate (sulfate reducers), and strict anaerobic organisms become the dominant species. Metabolism shifts from oxidative to fermentative under oxygen limiting soil conditions and becomes less efficient in terms of energy production and substrate utilization. The maximum rate of decomposition of degradable hazardous compounds is generally correlated with aerobic, oxidizing conditions. Excessive levels of degradable materials may lead to a depletion of oxygen and the formation of anaerobic, reducing conditions in the soil pores. The rate and extent of decomposition of many contaminants is limited under these reducing conditions, and anaerobic metabolism may result in reduced compounds that are odorous and toxic to microorganisms.

Subsurface oxygen concentration was measured under field conditions where petroleum waste was applied as part of a soil biodegradation field study at the Texaco Nanticoke oil refinery at Simcoe, Ontario, Canada. Dissolved oxygen sensors were placed at 6, 12, and 24 inches below the ground surface prior to application and incorporation of the refinery waste sludge. Subsurface sampling wells, ~1" in diameter, were hand augured into the soil, and 3/4" PVC Schedule 40 pipes, fitted with air tight o-ring seals, were placed into the wells. The wells were then backfilled with wet soil to ensure a tight seal around the outside of the pipe. Soil dissolved oxygen sensors (Jensen Instruments, Tacoma, WA) were lowered into the wells and snapped into the air tight seals. The sensors were connected to a programmable data measurement, collection, and logging device (Campbell Scientific, Logan, UT) that allowed continuous measurement of the oxygen content in the soil pores, averaging of the continuous readings over discrete sampling periods, and storage of the discrete O₂ levels on cassette tape for later processing on a microcomputer. Calibration of the probes was done in air at least daily, by removing the probes from the sampling wells, allowing them to equilibrate, and adjusting the amplifier output of the sensor so that the display reading corresponded to atmospheric levels of oxygen.

Dissolved oxygen sensors were put into service prior to waste application to collect background measurements of subsurface O₂ concentrations. Monitoring was continued during and after waste application. The full record of raw O₂ measurements is provided in Appendix D of this report. A subset of the data record was selected for study and comparison with VIP model simulation of soil oxygen dynamics at field scale.

MOISTURE

Soil water serves an important function as a transport medium through which nutrients diffuse and through which waste products are removed from the microbial cell surface. Soil water potential is the term used to express the energy with which water is associated with a soil surface and represents an energy potential against which organisms must work to extract water from the soil matrix. Microbial activity generally can be sustained at water potentials from -5 to lower than -15 bars without significant inhibition, while the lower

limit for bacterial activity is probably about -80 bars (Soil Science Society of America 1981). Fungi appear to be more tolerant of low soil water potential than bacteria (Gray 1978, Harris 1981), therefore microbial decomposition of organic materials in dry soils would be attributed primarily to fungal activity. Although some information exists regarding soil moisture effects on soil microbes, extensive information on optimal and marginal water potentials for growth, reproduction, and survival of individual species of microorganisms in soil remains limited (Taylor et al. 1980).

At saturation or near saturation conditions as soil pores become filled with water, the diffusion of gases through the soil is severely restricted, oxygen is consumed faster than it is replenished in the soil vapor phase, the soil becomes anaerobic, and major shifts in microbial metabolic activity occur. Changes in soil microbial metabolic activity can be correlated with oxidation-reduction potential, or Eh, which is an expression of the electron density of a system. Effects of high soil moisture content with regard to limiting diffusion of oxygen in the soil atmosphere have been discussed previously.

Experiments were conducted to determine the effect of soil moisture on the rate of apparent degradation of a subset of hazardous substances. Soil moisture levels of -0.33, -1.0, and -5.0 bars matric potential were used. Temperature was maintained at 20°C, and glass beaker reactors containing 200 g sandy loam soil were incubated in the dark to prevent photodegradation. Moisture was maintained at the desired levels by periodic addition of distilled water to each beaker and mixing with a glass stirring rod. Periodically through time triplicate sets of reactors at each soil moisture level were removed from incubation and solvent extracted with dichloromethane according to the method of Coover et al. (1987). Concentrations of PAHs in soil were determined by HPLC analysis of the extracts.

SOIL TYPE

Soil texture and clay mineralogy are also important factors affecting soil microbial processes (Stotzky 1972, 1980). Clays with a 1:1 crystal lattice, e.g., kaolinite are non-swelling and have low cation exchange capacity, while 1:2 crystal lattice clays, e.g., montmorillonite, swell, trapping water and dissolved materials between the lattices. The high cation exchange capacities of clays like montmorillonite greatly increase the buffer capacity at microsite within the soil, and reduces the impact of protons released into the soil environment as product of microbial metabolism. Differential sorption of organic compounds and inorganic ions by different clays also affects the availability of substrates and micronutrients to the soil microorganisms.

Soil organic matter is an important soil property that affects sorption as well as degradation (U.S. EPA, 1984 a and b). Sorbed compounds or ions may be available for extended periods of time for microbial metabolism and transformation if retained within the soil matrix by soil organic matter (Mahmood and Sims, 1986). Detailed discussion of the influence of soil organic and mineral components are presented elsewhere (U.S. EPA, 1984 a and b).

Soil pH is also an important soil property. The optimum pH range for rapid decomposition of most wastes and residues is from 6.5 to 8.5. Bacteria and actinomycetes have pH optima near neutrality, and do not compete with fungi in aqueous media, that are more tolerant to acidic conditions i.e., pH levels less than 5. Competition between fungi and other microorganisms as a function of pH is less clear in soils, however, where the buffer capacity of clay and humic materials affects the concentration of protons at the microsite scale (Gray 1978).

Two soil types, a McLaurin sandy loam and a Kidman sandy loam, were evaluated with regard to degradation and immobilization, or partitioning, of a subset of hazardous substances. The Kidman sandy loam soil (U.S. EPA 1988) was described previously in this section under temperature. McLaurin sandy loam properties include a soil pH of 4.8, 0.94% by weight organic carbon, 0.003% by weight total phosphorus, 0.02% by weight total nitrogen, and a saturation water content of 20% by weight. For biodegradation rate determination, selected substances were mixed with the two soils and incubated in glass beaker reactors at 20°C in the dark to prevent photodegradation. Moisture content was maintained at -0.33 bar matrix potential by periodic addition of distilled water to the soil in the glass reactors and mixing. Periodically through time triplicate sets of reactors containing each soil type were removed from incubation and solvent extracted with dichloromethane according to the procedure of Coover et al. (1987). Concentrations of chemicals were determined by HPLC analysis of the soil extracts.

Partition coefficients for a subset of substances were calculated for the two soil types using quantitative structure-activity relationships (QSARs). Partition coefficient for each chemical between soil and water, K_d , is given by:

$$K_d = \frac{C_s}{C_w} \quad [20]$$

where K_d is the soil/water partition coefficient (dimensionless if C_s and C_w are in the same units). C_s is the concentration of chemical in the soil phase, and C_w is the concentration of chemical in the aqueous phase. K_d values for organic substances can be estimated from K_{oc} (partitioning based upon soil organic matter) values if the organic fraction of the soil, f_{oc} , is known and if it is assumed that hydrophobic interactions dominate the partitioning processes:

$$K_d = K_{oc} \times f_{oc} \quad [21]$$

where K_{oc} is the organic carbon normalized soil/water partition coefficient.

By assuming that partitioning between water and the organic fraction of soil is similar to partitioning between octanol and water, a correlation equation can be used to relate K_{oc} to octanol/water partition coefficient (K_{ow}). The correlation equation used to calculate K_{oc} for this project was that of Karickhoff et al. (1979):

$$\log K_{oc} = 1.0 \log K_{ow} - 0.21 \quad [22]$$

Therefore using K_{ow} values it was possible to calculate K_{oc} for each chemical. Using the calculated K_{oc} and the measured organic carbon content for each experimental soil, the partition coefficient, K_d , was calculated.

SECTION 6

RESULTS AND DISCUSSION

SENSITIVE PARAMETERS

Temperature

Figures 2 through 15 present the trends observed for decrease in parent compound concentration with time of incubation for the PAH compounds evaluated (Coover, 1987). The percentages of each compound remaining in the soil at the end of the 240 day incubation period are presented in Table 2. Also presented are the estimated half-lives based on a first-order kinetic model for degradation and representative half-life values obtained from the literature.

The extent and rate of apparent loss was much greater for PAHs of low molecular weight and high aqueous solubility. Substantial loss of three-ring compounds acenaphthene, fluorene, and phenanthrene was observed at all temperatures during the course of the study. Four-ring compounds, including fluoranthene, pyrene, and benz[a]anthracene demonstrated greatly reduced rate of degradation under the temperature range from 10° to 30°. Loss of chrysene, a four-ring compound, and the remaining five and six-ring compounds was minimal at all three temperatures. Bossert et al. (1984) found similarly that after a 1280 day laboratory simulation of the land treatment process the total remaining of three-ring, four-ring, five-ring, and six-ring PAHs was 1.4, 47.4, 78.5, and 78.3% respectively. Other investigators have noted this general trend for the PAH class of compounds (Sims and Overcash 1983, PACCE 1985, Herbes and Schwall 1978).

Based upon the experimental results obtained for degradation rate as a function of temperature, the effects of temperature were described by the Arrhenius equation. The parameters for fluorene, anthracene, fluoranthene, pyrene and benz[a]anthracene are presented in Table 3. The Arrhenius expression may be appropriate for quantitatively describing the effect of temperature on PAH loss rates in soil for those PAH compounds where an effect of temperature is observed.

The sensitivity of the output of the mathematical model VIP was evaluated with respect to the effect of temperature on degradation rate for a subset of PAH compounds. Presentation and discussion of these results is presented in a subsequent subsection Model Output as a Function of Temperature-dependent Degradation.

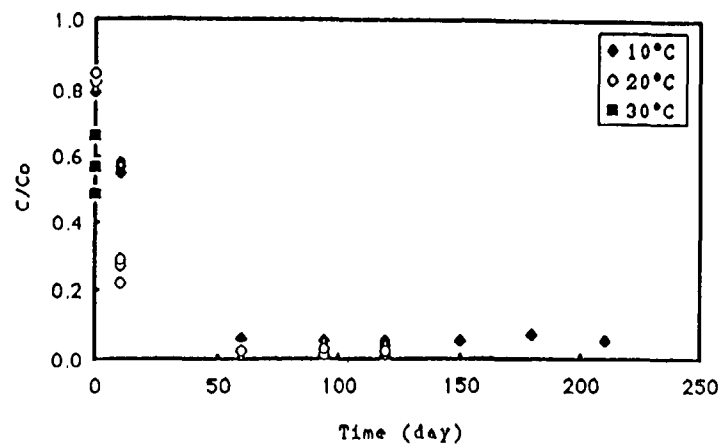


Figure 2. Apparent Loss of Acenaphthene

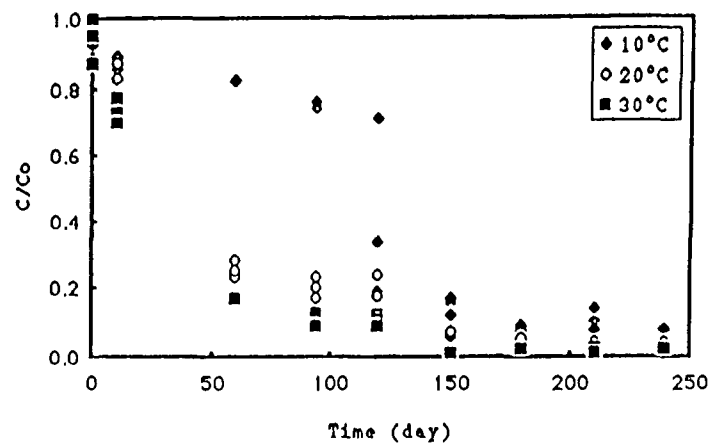


Figure 3. Apparent loss of Fluorene

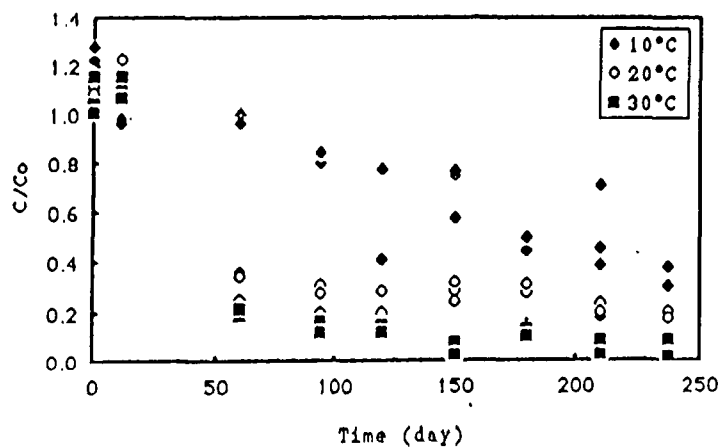


Figure 4. Apparent Loss of Phenanthrene

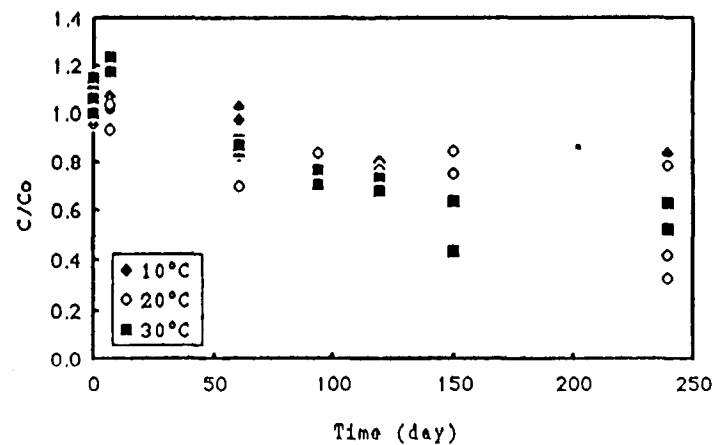


Figure 5. Apparent Loss of Anthracene

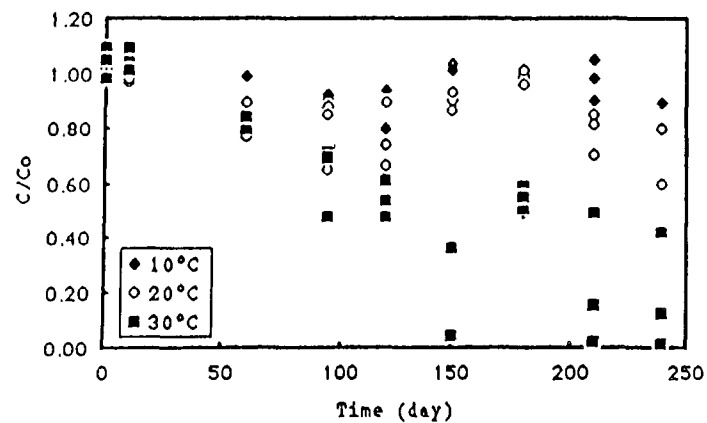


Figure 6. Apparent Loss of Fluoranthene.

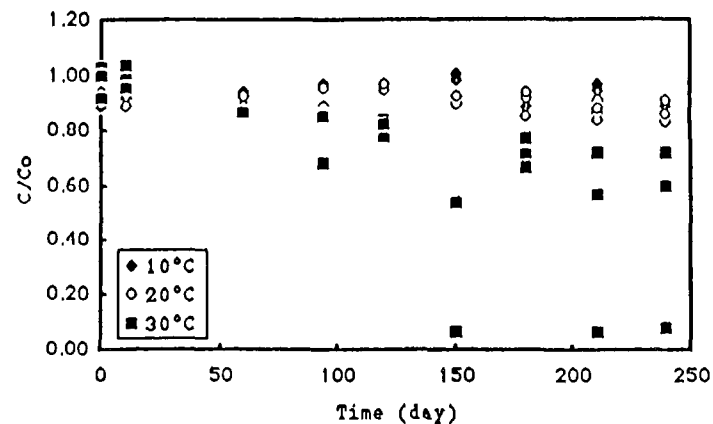


Figure 7. Apparent Loss of Pyrene.

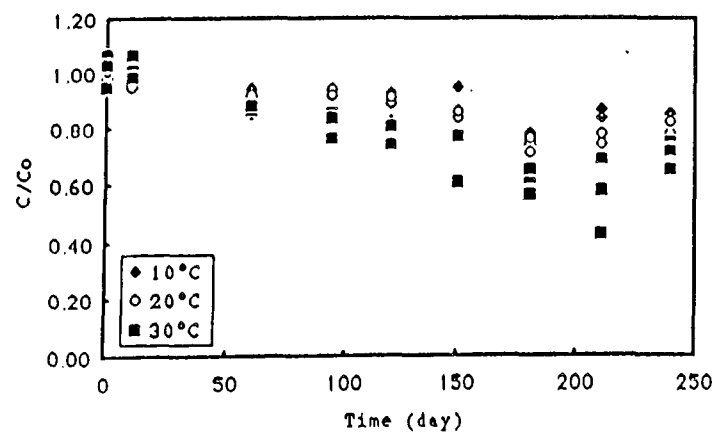


Figure 8. Apparent Loss of Benz[a]anthracene.

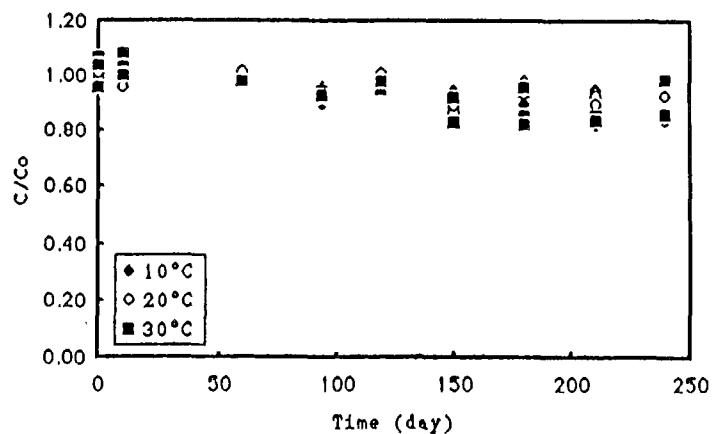


Figure 9. Apparent Loss of Chrysene.

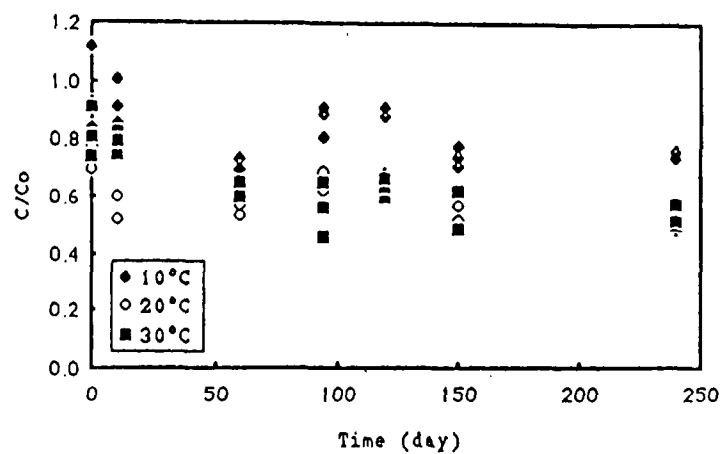


Figure 10. Apparent Loss of Benzo[a]pyrene

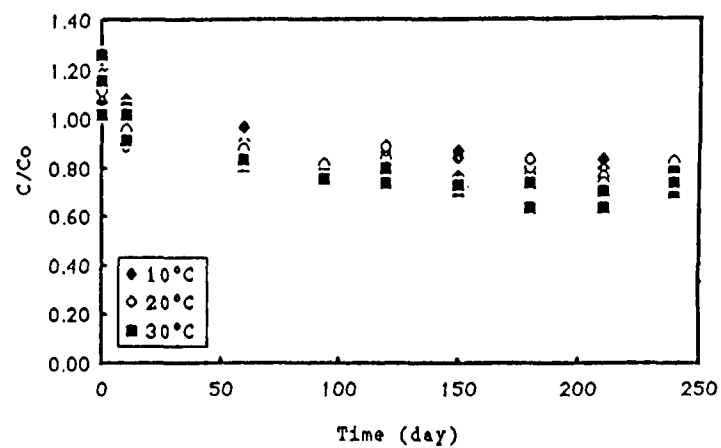


Figure 11. Apparent loss of Benzo[b]fluoranthene

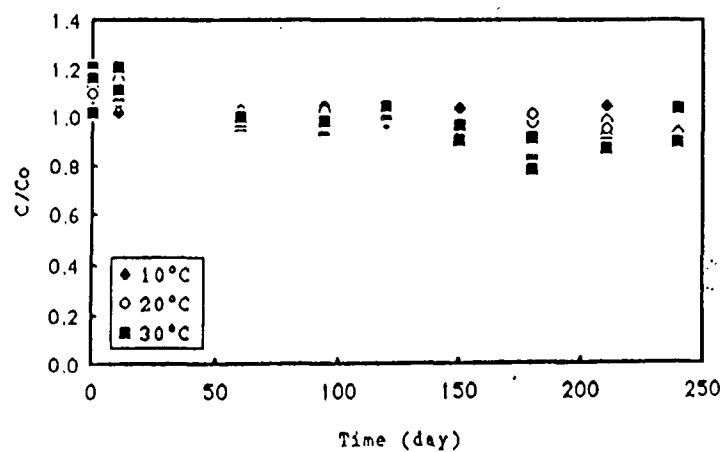


Figure 12. Apparent Loss of Benzo[k]fluoranthene

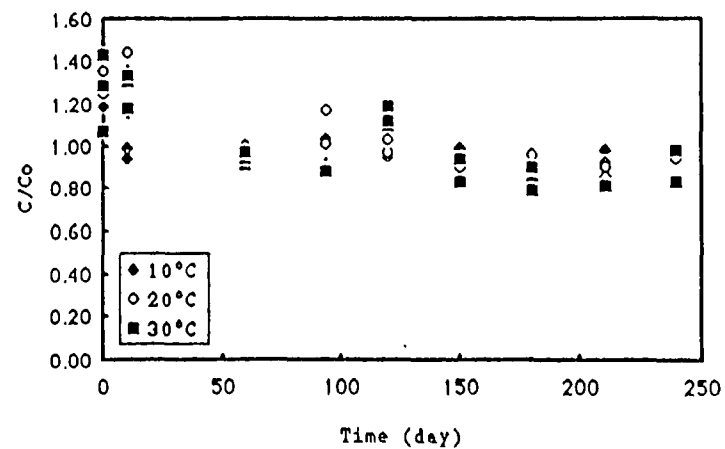


Figure 13. Apparent Loss of Dibenz[a,h]anthracene

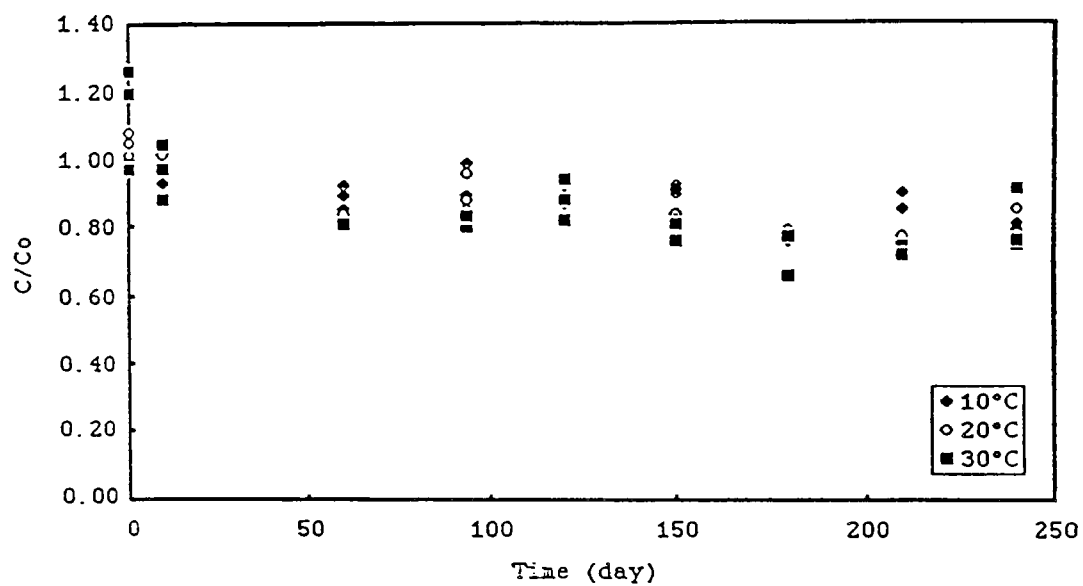


Figure 14. Benzo[g,h,i]perylene degradation.

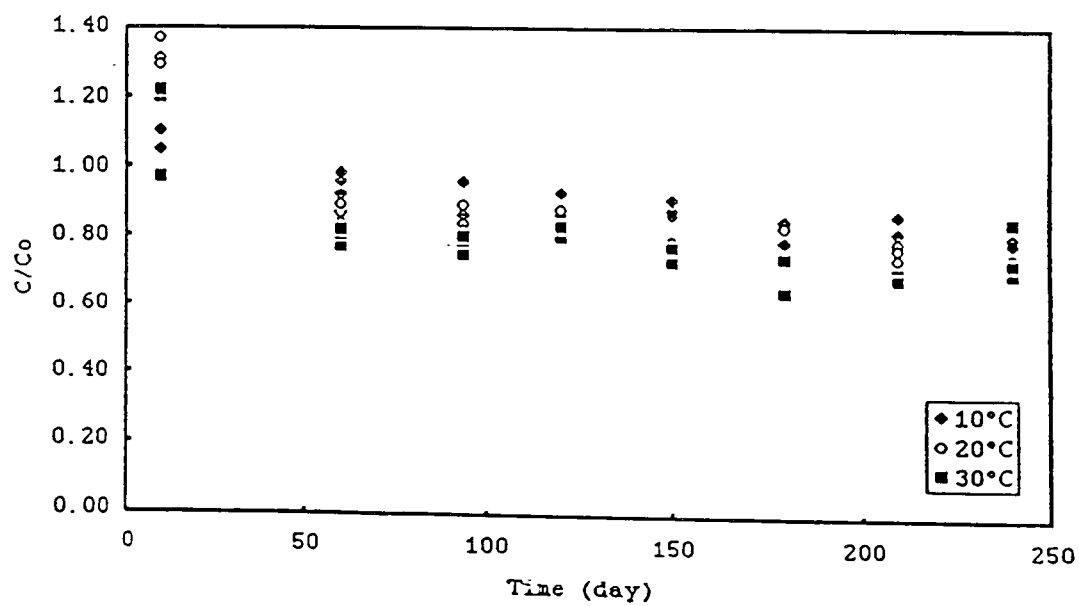


Figure 15. Indeno[123-c,d]pyrene degradation.

Table 2
Percentages of PAH Remaining at the End of the 240 Day Study Period and
Estimated Apparent Loss Half Lives

Compound	Per cent of PAH Remaining			Estimated Half Life (day) ^a			Half lives reported in the literature (day)
	10°C	20°C	30°C	10°C	20°C	30°C	
Acenaphthene	5	0	0	<60	<10	<10	96 ^b ,45 ^b ,0.3-4 ^c
Fluorene	8	3	2	60 (50-71)	47 (42-53)	32 (29-37)	64 ^b ,39 ^b ,2-39 ^c
Phenanthrene	36	19	2	200 (160-240)	<60	<60	69 ^b ,23 ^b ,26 ^c ,9.7 ^d ,14 ^d
Anthracene	83	51	58	460 (320-770)	260 (190-420)	200 (170-290)	28 ^b ,17 ^b ,108-175 ^c ,17 ^d ,45 ^d
Fluoranthene	94	71	15	f	440 (280-1000)	140 (120-180)	104 ^b ,29 ^b ,44-182 ^c ,39 ^d ,34 ^d
Pyrene	93	89	43	f	1900 (1100-8100)	210 (150-370)	73 ^b ,27 ^b ,3-35 ^c ,58 ^d ,48 ^d
Benz[a]anthracene	82	71	50	680 (520-980)	430 (360-540)	240 (200-280)	52 ^b ,123 ^b ,102-252 ^c ,240 ^d ,130 ^d
Chrysene	85	88	86	980 (710-1500)	1000 (750-1900)	730 (550-1100)	70 ^b ,42 ^b ,5.5-10.5 ^c ,328 ^d ,224 ^d
Benzo[b]fluoranthene	77	75	62	580 (400-1100)	610 (410-1200)	360 (280-510)	73-130 ^e ,85 ^b ,65 ^b
Benzo[k]fluoranthene	93	95	89	910 (640-1600)	1400 (840-5700)	910 (500-5310)	143 ^b ,74 ^b
Benzo[a]pyrene	73	54	53	530 (300-2230)	290 (170-860)	220 (160-380)	91 ^b ,69 ^b ,30-420 ^c ,347 ^d ,218 ^d
Dibenz[a,h]anthracene	88	87	83	820 (520-1920)	750 (490-1600)	940 (490-12940)	74 ^b ,42 ^b ,100-190 ^e
Benzo[g,h,i]perylene	81	76	75	650 (420-1300)	600 (410-1170)	590 (340-2390)	179 ^b ,70 ^b
Indeno[1,2,3-c,d]pyrene	80	77	70	600 (450-910)	730 (460-1830)	630 (350-3130)	57 ^b ,42 ^b ,200-600 ^e

^a $t_{1/2}$ (95 per cent confidence interval)

^b Sims (1986), T=20°C

^c Sims and Overcash (1983), T=15-25°C

^d PACCE (1985), T=20°C

^e Sims (1982), T=20°C

^f Least squares slope (for calculation of $t_{1/2}$) = zero with 95% confidence

Table 3. Arrhenius parameters for the apparent loss of PAH compounds in sandy loam soil.

Compound	Activation Energy (Kcal/mol)	Preexponential Term $\ln(A)^*$	Kinetic Model
Fluorene	5.0	4.5	first
Anthracene	7.5	12.9	zero
Fluoranthene	21.7	36.3	zero
Pyrene	40.3	67.0	zero
Benz[a]anthracene	9.4	12.8	zero

* A has units of $\mu\text{g/g/d}$ for zero order model and $1/\text{d}$ for the first order model.

Moisture

Results for the effects of soil moisture at 20°C on the rate of degradation of subset of PAH compounds, incubated in soil as a synthetic mixture of the PAHs shown, are expressed in terms of half-life values and 95% confidence intervals (CI) on half-life values in Table 4. Half-life values were calculated based on a first-order model for PAH disappearance.

Degradation rates were significantly different at different soil moisture levels for the three-ring PAH anthracene and the four-ring PAH fluoranthene. For the PAH compounds naphthalene (two-ring), phenanthrene (three-ring), and pyrene (four-ring), no significant effect of soil moisture was evident. Because of the

Table 4. The effect of soil moisture on degradation rate of PAH compounds in sandy loam soil

Compound	20-40% F.C.*		40-60% F.C.		60-80% F.C.	
	$t_{1/2}$ (days)	95% CI	$t_{1/2}$ (days)	95% CI	$t_{1/2}$ (days)	95% CI
Naphthalene	30	15- 93 a ⁺	28	14- 93 a	33	18- 23 a
Anthracene	72	50-128 a	46	27-173 a	18	7- 46 b
Phenanthrene	79	53-154 a	-	-	58	72-147 a
Fluoranthene	530	462-578 a	200	165-267 b ⁺	230	193-289 b
Pyrene	-	-	7500	877- ∞ a	5300	2500- ∞ a

* F.C. = field capacity of the soil.

⁺ The same letter (a or b) for a compound at two moisture contents indicates no statistical difference at the 95% level based on a t-test.

lack of a rational quantitative relationship between soil moisture content and rate of degradation, it was not possible to evaluate the mathematical model VIP with regard to model output as a function of soil moisture.

Soil Type

Results for degradation rates, corrected for volatilization, for a subset of PAH compounds and eight pesticides incubated individually at -0.33 bar soil moisture and 20°C, as a function of soil type are presented in Table 5. Half-life values were calculated based on a first-order kinetic model for degradation; 95% confidence intervals (CI) are also given.

As indicated in this table, for the PAH compounds investigated, there was no statistically significant difference in degradation rate as a function of soil type

Table 5. Degradation rates corrected for volatilization for PAH compounds and pesticides applied to two soils.

Compound	Kidman Sandy Loam		McLaurin Sandy Loam	
	$t_{1/2}$ (days)	95% CI	$t_{1/2}$ (days)	95% CI
PAHs:				
Naphthalene	2.1	1.7-2.7 a ⁺	2.2	1.7-3.4 a
1-Methyl-naphthalene	1.7	1.4-2.1 a	2.2	1.6-3.2 a
Anthracene	134	106-182 a	50	42-61 b ⁺
Phenanthrene	16	13-18 a	35	27-53 b
Fluoranthene	377	277-587 a	268	173-630 a
Pyrene	260	193-408 a	199	131-408 a
Chrysene	371	289-533 a	387	257-866 a
Benz[a]anthracene	261	210-347 a	162	131-217 a
7,12-Dimethyl- benz[a]anthracene	20	18-24 a	28	21-41 a
Benzo[b]fluoranthene	294	231-385 a	211	169-277 a
Benzo[a]pyrene	309	239-462 a	229	178-315 a
Dibenz[a,h]anthracene	361	267-533 a	420	267-990 a
Dibenzo[a,i]pyrene	371	277-533 a	232	178-330 a
Pesticides:				
Phorate	32	29-85 a	24	19-35 a
Aldicarb	385	257-845 a	30	27-35 b
Pentachloronitrobenzene	17	15-21 a	51	38-74 b
Lindane	61	35-257 a	65	39-204 a
Heptachlor	58	50-70 a	63	58-76 a
Famphur	53	46-69 a	69	58-98 a
Dinoseb	103	87-128 a	92	74-124 a
Pronamide	96	81-122 a	94	69-151 a

⁺ The same letter for a compound at two soil types indicates no statistical difference at the 95% level based on a t-test.

for the majority of PAHs. Although a statistically significant difference was observed for anthracene and phenanthrene, the difference was not consistent for one soil type.

For the pesticides evaluated, there were statistically significant differences for degradation rates as a function of soil type for pentachloronitrobenzene and aldicarb. For the other six pesticides no statistical difference in degradation rate was observed between the two soil types. Because of the lack of a rational quantitative relationship between soil type and rate of degradation, it was not possible to evaluate the test model with regard to model output as a function of soil type.

Partition coefficients between aqueous and solid phases (K_d) for each soil type, derived using structure-activity relationships (SAR), are presented in Table 6. Calculated values presented indicate a consistent difference between the soils, with K_d values higher for chemicals in McLaurin Sandy Loam soil. Since the values are calculated and not measured, 95% confidence intervals are not relevant. The difference between the two soils is directly related to the difference in organic carbon content for the two soils (0.5% for Kidman soil versus 0.94% for McLaurin soil).

MODEL OUTPUT AS A FUNCTION OF TEMPERATURE-DEPENDENT DEGRADATION

The proper design and management of a hazardous waste land treatment system requires an understanding of the rates at which hazardous constituents of an applied waste are degraded. Temperature is the most important climatic factor influencing rates of decomposition in soils (Smith, 1982). Coover (1987) has conducted laboratory scale experiments using glass beaker studies for 16 PAH compounds that are representative of hazardous wastes of concern to the U.S. Environmental Protection Agency. All experiments were conducted at three temperatures (10°C, 20°C, and 30°C) using a Kidman sandy loam soil. Coover (1987) indicated that the Arrhenius expression, $k = A e^{(E_a/RT)}$, was useful for describing the effects of temperature on apparent loss of fluorene, anthracene, and benz[a]anthracene and other PNAs, but found that its use should be justified on a case-by-case basis.

In the VIP model, a degenerate form of the Arrhenius expression is found by integrating the differential form between the limits T_1 and T_2 :

$$\ln \left(\frac{K_1}{K_2} \right) = \frac{E_a(T_1 - T_2)}{RT_1T_2} \quad [23]$$

and restricting the temperature range to ± 10 -15°C, as is the case for most vadose zone environments. The Eq.[23], K_1 and K_2 are the rate constants at T_1 and T_2 , E_a is the activation energy, and R is the gas constant. Under this restriction, the term E_a/RT_1T_2 remains approximately constant, and Eq.[23] may be written as

$$\ln \left(\frac{K_1}{K_2} \right) = \theta^\circ (T_1 - T_2). \quad [24]$$

Table 6. Calculated soil/water (Kd), partition coefficients for chemicals in two soils.

Compound	log Kd (McLaurin)	log Kd (Kidman)
Acenaphthylene	1.72	1.38
Benz[a]anthracene	3.24	2.90
Benzo[a]pyrene	3.67	3.33
chrysene	3.24	2.90
Dibenzo[a,h]anthracene	3.60	3.26
Ideno(1,2,3-cd)pyrene	5.27	4.93
3-Methylcholanthrene	4.73	4.38
Fluoranthene	2.97	2.62
1-Methylnapthalene	1.52	1.18
Naphthalene	1.01	0.67
Phenanthrene	2.11	1.76
Pyrene	2.96	2.61
Benzo[b]fluoranthene	4.19	3.86
7,12-Dimethylbenz[a]anthracene	3.61	3.27
Anthracene	2.10	1.75
Bis-(chloromethyl) ether	-2.68	-3.02
Chloromethyl methyl ether	-1.41	-1.75
1,2-Dibromo-3-chloropropane		
Dichlorodifluoromethane	-0.17	-0.51
1,1-Dichloroethylene		
1,1,1-Trichloroethane	0.13	0.47
1,1,2,2-Tetrachloroethane	2.63	2.29
1,1,2-Trichloroethane	-0.16	-0.50
1,2,2-Trichlorotrifluoroethane	-0.66	-1.01
Hexachlorocyclopentadiene	2.68	2.34
4,4-Methylene-bis(2-chloroaniline)	0.96	0.62
1,2,4-Trichlorobenzene	1.63	1.29
Aldrin	0.65	0.31
Cacodylic Acid	-2.31	-2.65
Chlordane, technical	0.44	0.10
DDT	1.14	0.79
Dieldrin	0.56	0.22
Disulfoton	-2.31	-2.65
Endosulfan	1.21	0.86
Heptachlor	1.55	1.21
Alpha Lindane	1.46	1.12
Methyl parathion	0.65	0.31
Parathion	1.06	0.72
Phorate	0.58	0.24
Toxaphene	0.96	0.62
Warfarin	0.19	-0.15
Aldicarb	-1.61	-1.95

Taking antilogs

$$\frac{K_1}{K_2} = e^{\theta \cdot (T_1 - T_2)} = \theta^{(T_1 - T_2)} \quad [25]$$

where $\theta = e^{\theta'}$. This form has been used to characterize the effect of temperature on soil biochemical degradation and mineralization of some compounds in soils (Hamaker, 1972 and Parker, 1983). Using $T_2 = 20^\circ\text{C}$,

$$K_T = K_{20} \theta^{(T-20)} \quad [26]$$

where K_T is the constituent degradation rate at temperature $T^\circ\text{C}$, K_{20} is the constituent degradation rate at 20°C , and θ is the temperature correction coefficient.

The method of non-linear least squares was used to estimate the degradation rate at 20°C (K_{20}) and the temperature correction coefficient value (θ) of Eq.[26] for three PNA compounds: chrysene, benzo[b]fluoranthene, and fluorene, using the data of Coover (1987). Appendix A provides the temperature data and the parameter estimation for these three compounds. The concentration histories and the predicted first order models are shown in Figures 16 a, b, and c, for chrysene, benzo(b)fluoranthene, and fluorene respectively. The estimated K_{20} and θ and their 95% confidence intervals are listed in Table 7. Note that for chrysene, the 95% CI for θ includes one, so that, for these data, there is no statistically significant effect of temperature on apparent degradation.

Simulations using these three compounds were run using the VIP model to evaluate the effects of soil temperature on model predictions. Partition coefficients and soil initial concentrations of three compounds used in this study are summarized in Table 8. For this series of runs, a high recharge rate $3.95 \text{ (cm}^3\text{/day/cm}^2\text{)}$ was used, and the mass transfer rate coefficients for the constituents and oxygen were 1000 day^{-1} , assuming the constituents and oxygen reached equilibrium very rapidly.

Table 7. Estimated values of K_{20} and θ .

Compound	LCL ^a (1/days)	K_{20} (1/days)	UCL ^b (1/days)	LCL	θ	UCL
Chrysene	0.00046	0.00059	0.00072	0.987	1.003	1.019
Benzo[b]fluoranthene	0.00144	0.00168	0.00192	1.012	1.024	1.036
Fluorene	0.0159	0.0168	0.0178	1.033	1.040	1.048

^a Lower 95% confidence limit

^b Upper 95% confidence limit

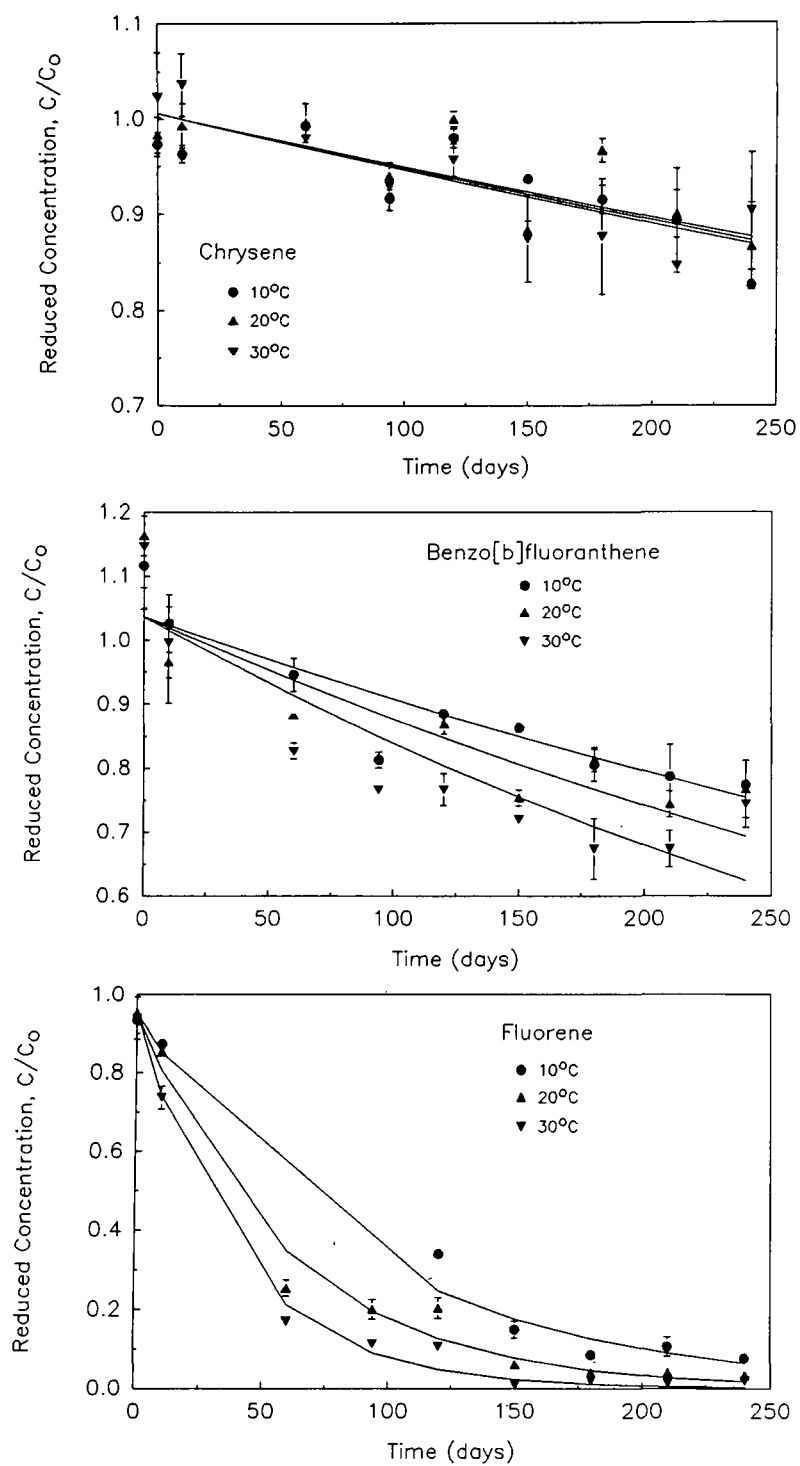


Figure 16. Concentration histories and the predicted first order models for chrysene, benzo[b]fluoranthene, and fluorene. Model predictions (—) decrease with increasing temperature.

Table 8. Partition coefficients and initial concentrations used in the study.

Compound	K_{ow} g/m ³ /g/m ³	K_{sw} g/g/g/m ³	K_{aw} g/m ³ /g/m ³	Initial mg/g-soil
Chrysene	8.9E+5 ^a	1.8E-4 ^b	3.9E-3 ^a	0.1 ^a
Benzo[b]fluoranthene	1.1E+7 ^a	4.9E-5 ^b	1.2E-3 ^a	0.04 ^a
Fluorene	2.0E+3 ^b	6.2E-5 ^b	3.2E-3 ^c	0.1 ^d

^a From U.S. EPA (1988).^b From Ryan et al. (1987).^c Calculated from Henry's Law.^d Coover (1987).

Table 9 lists the summary of degradation data of the three compounds after a one year simulation in the Kidman sandy loam. The extent and rate of apparent loss due to the biochemical degradation for the higher temperature is greater than that for the lower temperature for each of the three compounds studied. However, the effect of temperature on the apparent loss from decay is different for each compound, ranging from 20 percent for chrysene to 100 percent loss for fluorene at 30°C.

Table 9. Degradation summary from VIP simulation.

Compound	Temp. °C	% decayed	total mass g
Chrysene	10	19	26
	20	19	
	30	20	
Benzo[b]fluoranthene	10	38	10
	20	45	
	30	53	
Fluorene	10	98	26
	20	100	
	30	100	

Figure 17 through 19 demonstrate the depth profiles of chrysene, benzo[b]fluoranthene, and fluorene, respectively, in the water phase after one year in the Kidman sandy loam. Compared to the profiles for benzo[b]fluoranthene (Figure 18) and fluorene (Figure 19), for chrysene there is little apparent effect of temperature seen in these profiles with temperature changing from 10 to 30°C. The plot for fluorene (Figure 19) shows the largest apparent effect of temperature on the model output profiles. The effect of temperature on the degradation rate depends on the value of θ . Higher values of θ (1.040 for fluorene), show more sensitivity to temperature in the model prediction than that for θ values close to 1.0 (1.003 for chrysene). This result is in agreement with the mathematical aspect of Eq. [26].

Fluorene has a low molecular weight of 166 and only three fused rings, while benzo[b]fluoranthene and chrysene have five and four rings respectively. Figures 17 to 19 and Table 9 demonstrate that the extent and rate of degradation of low molecular weight PAH compounds increased with increasing soil temperature, but there was very little apparent degradation and little effect of temperature on degradation of four and five-ring compounds. Therefore, the high molecular weight PAHs have the potential to persist for years and have a potential to accumulate following repeated addition of PAH-containing wastes in land treatment systems. These results predicted from the test model are in agreement with observations of Coover (1987) observed in laboratory scale experiments.

MODEL OUTPUT AS A FUNCTION OF OXYGEN-LIMITED DEGRADATION

Simulations were conducted to evaluate the effects of oxygen concentration on the degradation of the constituent. The physical and kinetic parameters used in this test are contained in Table 10. For this series of runs, the dispersion coefficient for oxygen, D_{ao} , was set to zero to maximize the potential for O_2 limitation by restricting oxygen sources.

Figure 20 shows a comparison of the concentration distribution with and without oxygen-limits after 80 days in the water phase. The results demonstrate that there is no significant difference between the concentration curves with oxygen-limit degradation. The reason is that the oxygen half saturation constant used was 0.1 g/m³ which is very small compared to the oxygen concentrations 200-298 g/m³ in the air phase and 4-9.17 g/m³ in the water or oil phase. This small value of the oxygen half saturation constant caused the term, $O/(K_o+O)$ to approach unity. Therefore degradation would not be affected by the concentration of oxygen. When the oxygen half saturation constant value increases to a value near the oxygen concentration, an increased sensitivity of degradation to the oxygen concentration would be expected.

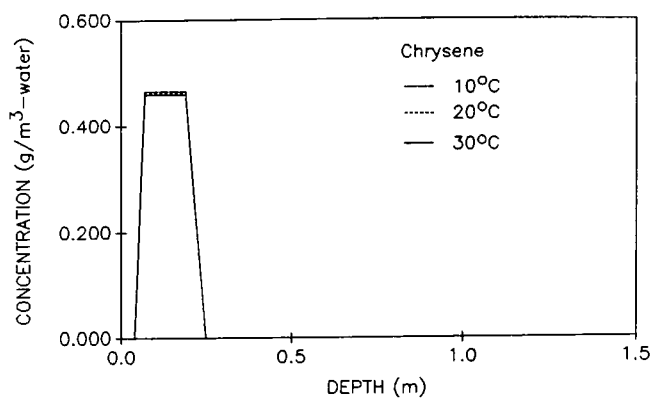


Figure 17. Depth profiles of chrysene at three different temperatures after one year.

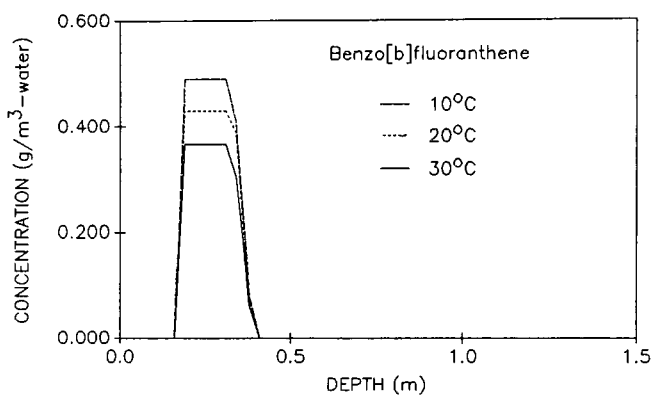


Figure 18. Depth profiles of benzo[b]fluoranthene at three different temperatures after one year.

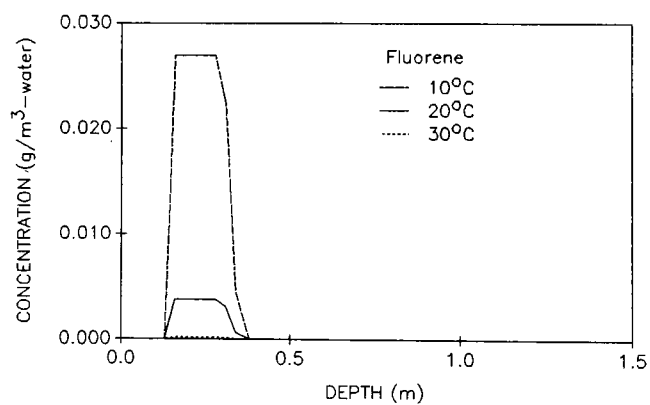


Figure 19. Depth profiles of fluorene at three different temperatures after one year.

Table 10. Physical and kinetic parameters used in model simulation of oxygen dynamics at field scale.

μ_w	constituent degradation rate in the water phase, day ⁻¹	0.0147 ^d
μ_s	constituent degradation rate in the soil phase, day ⁻¹	0.0147 ^d
K_{sw}	constituent partition coefficient between soil phase and water phase (g/g-soil)/(g/m ³ -water)	3.16E-6 ^d
K_a	oxygen half saturation constant in the air phase, g/m ³	0.1 ^a
K_o	oxygen half saturation constant in the oil phase, g/m ³	0.1 ^a
K_w	oxygen half saturation constant in the water phase, g/m ³	0.1 ^a
K_{oo}	oxygen half saturation constant with respect to the oil decay g/m ³	0.1 ^a
K_{oa}	oxygen partition coefficient between the oil and air phases, (g-O ₂ /m ³ -oil)/(g-O ₂ /m ³ -air)	0.0306 ^{be}
K_{wa}	the oxygen partition coefficient between the water and air phases, (g-O ₂ /m ³ -water)/(g-O ₂ /m ³ -air)	0.0306 ^b
ν_c	the stoichiometric ratio of the oxygen to the constituent consumed	3
ν_o	the stoichiometric ratio of the oxygen to the oil consumed	3
κ_o^a	the oxygen transfer rate coefficient between the oil and air phases, day ⁻¹	1000 ^c
κ_w^a	the oxygen transfer rate coefficient between the water and air phases, day ⁻¹	1000 ^c
V_w'	mean daily recharge rate, (cm/day)	4.30 ^d
c	saturated hydraulic conductivity (cm/day)	100
ϕ	soil porosity (cm ³ /cm ³)	0.39

^a From Borden and Bedient (1986).

^b Calculated from Henry's Law.

^c Assume oxygen reaches equilibrium very fast.

^d From Grenney et al. (1987).

^e Assume oxygen partition coefficient between the oil and air phase is same as that between the water and air phase.

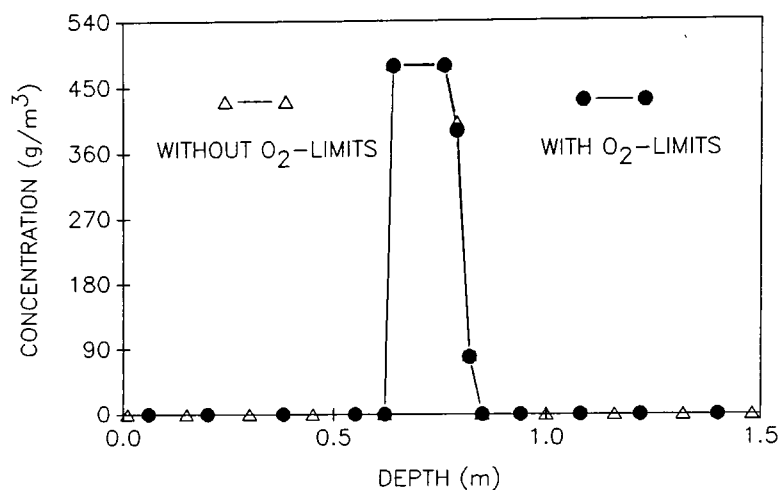


Figure 20. Comparison of the depth profiles with and without oxygen-limits.

Figure 21 presents the constituent and oxygen concentration curves in the water phase after 80 days. The soil system is saturated with oxygen from the top of the soil surface down to a soil depth where the constituent slug is located. The oxygen concentration decreases over these depths due to the oxygen demand imposed by microbial degradation of the constituent. No microbial activity has occurred below the constituent wave front, therefore the oxygen concentration is maintained at the saturation concentration.

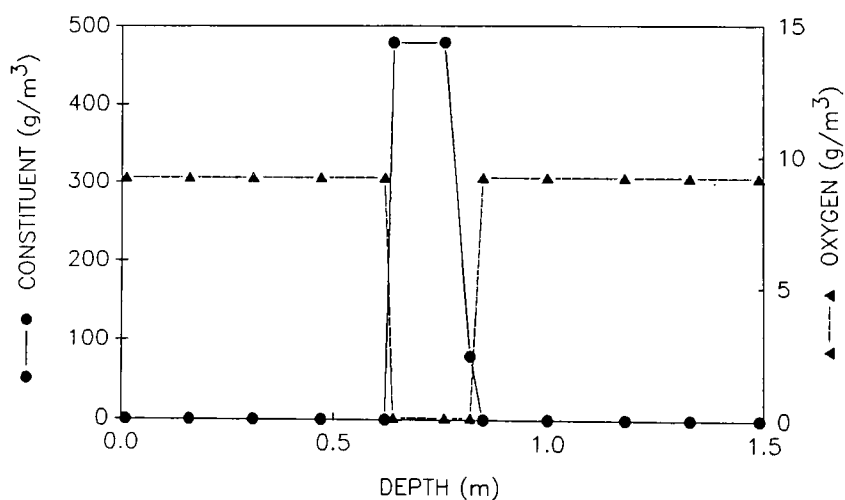


Figure 21. Constituent and oxygen profiles after 80 days.

Figure 22 shows the breakthrough curves of the constituent and oxygen concentration in the water phase at a depth of 1.0 meter. The oxygen concentration decreases when constituent passes this depth due to microbial degradation of the constituent. After the constituent slug passes a particular depth, the oxygen concentration is replenished due to the advection transport mechanism in the air and water phases.

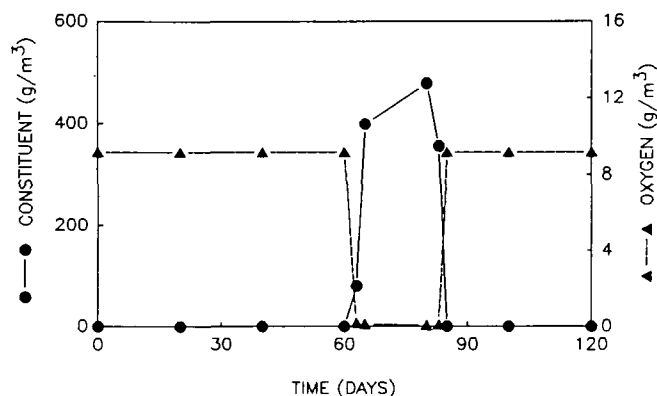


Figure 22. Constituent and oxygen breakthrough curves predicted by the VIP model.

Figure 23 shows the effect of the half-saturation constant for the same input data set, for a range of K from 0.01 to 10 g/m^3 in the air, oil, and water phases. These simulations demonstrate that, as the value of this constant increases, the oxygen-limitation of degradation increases, as would be expected.

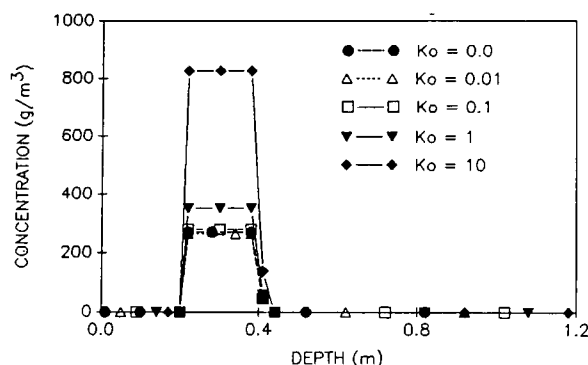


Figure 23. Depth profiles with five of half oxygen saturation constant coefficients.

Under field conditions, where O_2 is replenished by dispersion/diffusion from the atmosphere, this rate limitation will be less severe over the long term for slowly degradable substrates. However, for short term dynamics, such as immediately after a waste application, the O_2 limits may be very important and, therefore represent an important module (oxygen dynamics) for inclusion in the model. Evidence for the field scale depletion of soil oxygen, with depth through the soil, after waste application was confirmed at Texaco's Nanticoke Oil Refinery, Ontario, Canada, and is discussed in the next section.

FIELD EVALUATION OF MODEL FOR PREDICTION OF OXYGEN DYNAMICS

A field study was conducted as part of a land treatment demonstration for Texaco's Nanticoke Oil Refinery at Simcoe, Ontario, Canada. USU's involvement in the project was to characterize the waste being applied under two loading scenarios (high and low), and to evaluate the dynamics of the vapor phase processes for ten days following the application and tilling of the waste sludge, including volatile organic constituents and oxygen. Details of the study are provided in a separate report. Our purpose here is to briefly describe the measurement of subsurface oxygen concentration and to use the VIP model to simulate the short term dynamics of the oxygen in the subsurface.

The measurements from the high-load plot from the period 6/11/87-6/15/87 were chosen for the simulation. For the purposes of the simulation, the waste constituents were summed and assumed to be representable by a single constituent having fate, transport, and degradation properties that were averages of those for the individual materials. It should be noted that the averaging process was not rigorous: the values used were simple arithmetic averages of representative values taken from land treatment studies done at USU. These parameters, soil-water, octanol-water, and air-water partition coefficients and first order degradation rate coefficients, were entered into the VIP model with the initial conditions taken from the background measurements, and waste characteristics and application rates from field notes. The input file is shown in Table 11.

The model was run for the 5 day period of the data record. The predicted air phase O_2 concentrations at the 6 inch, 12 inch, and 24 inch depths were extracted from the model output and plotted alongside the raw field data. Results are presented in Figures 26, 27, and 28, for 6 inch, 12 inch, and 24 inch depths, respectively. The solid lines on the plots represent the model simulation, and the dashed lines represent the field data.

Results for the 6 inch depth show good agreement between the model prediction and the field data during the first 80 hours of the simulation. The model was able to track the descending leg of the record but is unable to simulate the recovery of the O_2 content at this level after 80 hours. For the 12 inch depth, the model was able to predict the general behavior of the data for 60 hours but was unable to predict the recovery after this time. At a depth of 24 inches, the model was able to predict the initial drop in the O_2 level, but the predicted trend continued to descend while the field data leveled off. However, at 60 hours, when the O_2 had decreased to about 25 g/m^3 , the model and data agreed. However, the test model failed to predict the recovery after about 80 hours.

Table 7 Input Data File for Simulation of Field Data from Nanticoke Refinery

[illegible]

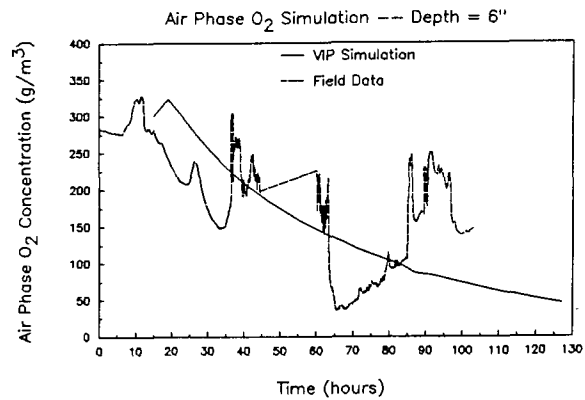


Figure 24. Oxygen simulation at depth 6".

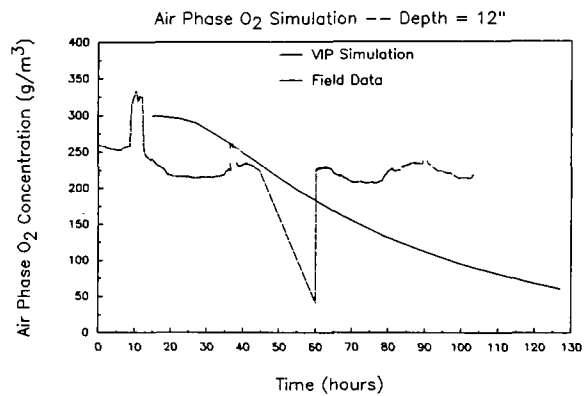


Figure 25. Oxygen simulation at depth 12".

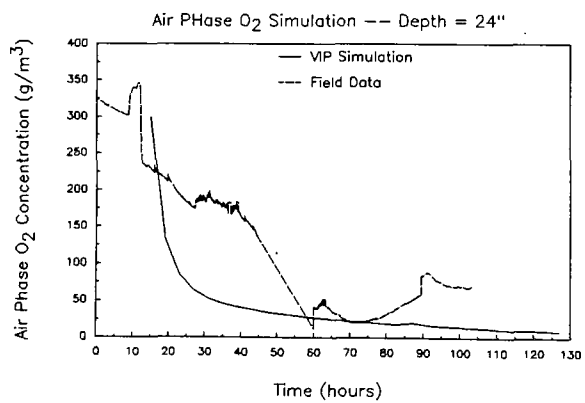


Figure 26. Oxygen simulation at depth 24".

The inability of the test model to predict the recovery of the O_2 levels after about 80 hours is felt to be related to the boundary conditions at the bottom of the treatment zone. For the simulations presented, it was assumed that the treatment zone extended to the 24 inch level. Below that level the soil was assumed to be saturated with water, and therefore no oxygen could be transported from below. A more realistic condition for this physical system, for which the groundwater was well below the 24 inch level, is a boundary that permits free transport of vapor. This would provide an oxygen source from below and would make the O_2 concentration decrease more slowly at this level, and also provide an oxygen source for recovery.

The VIP model therefore was useful for simulating the short term dynamics of O_2 after waste application. The model predicted the location of the decrease in the air phase O_2 concentration, and semi-quantitatively predicted the concentrations. More precise characterization of model inputs would make predictions more quantitative. The model failed, however, to predict the recovery of the O_2 concentrations at all levels after about 80 hours. Reformulation of the boundary conditions at the bottom of the treatment zone may improve the simulation.

ANALYTICAL SOLUTION TO TWO-PHASE MODEL

Analytical Solution

In this section, we discuss the analytical solution of the equations for a two-site model with first adsorption kinetics. This model has been studied extensively in a series of papers by S. Goldstein, which appeared in the 1950's (Goldstein, 1953a,b and 1959a,b,c). In addition to giving an analytical solution to the equations, Goldstein investigates the relationship between the equilibrium model and the kinetic model and gives asymptotic expansions for the solutions. For the convenience of the reader, we will outline the construction of an integral representation for the model under consideration in this report. Our approach is based on an application of the Riemann method to a form of the telegraph equation which arises in the course of the analysis of the model equations.

In order to simplify the presentation somewhat, we will first obtain a dimensionless version of the model equations by introducing dimensionless variables for the variables and the experimental parameters. In order to distinguish between the dimensional terms and their dimensionless counterparts, we will indicate dimensional terms with an * and the dimensionless terms will be written without the * (note: this does not correspond with the use of dimensional variables in the remainder of this report). The set of equations for the model problem can be written in the form of the following one-dimensional partial differential equation.

$$\frac{\partial C^*}{\partial t^*} + (\rho^*/\theta) \frac{\partial S^*}{\partial t^*} = -V_w^* \frac{\partial C^*}{\partial x^*} - \mu_w^*/\theta_w^* C^* \quad [27a]$$

$$-\infty < x^* < \infty, \quad 0 < t^* < \infty$$

$$\frac{\partial S^*}{\partial t^*} = \kappa^*(K_{sw}^* C^* - S^*) - \mu_s^* S^* \quad [27b]$$

with initial conditions

$$\begin{aligned} C^*(x^*, 0) &= f^*(x^*) \\ S^*(x^*, 0) &= g^*(x^*) \end{aligned} \quad -\infty < x^* < \infty$$

where

C^* is the concentration of the chemical in solution (g/m³),
 S^* is the amount of chemical sorbed per gram of soil (g/g),
 V_w^* is the vertical pore-water velocity (m/day),
 ρ^* is bulk density of the soil (g/m³),
 θ_w^* is the saturated water content (m³/m³),
 x^* is the depth, positive downward (m),
 t^* is time (days),

In the above equations, S^* and θ_w^* are already dimensionless. We will take the following as dimensionless variables:

$$\begin{aligned} C &= K_{sw}^* C^*, \\ x &= x^*/L^*, \text{ and} \\ t &= V_w^* t^*/L^* \end{aligned}$$

where L^* is an empirical scaling parameter (in our system, L^* is the depth of the initial treatment zone). Combining the above identifications into the system of equations results in the following Cauchy Problem.

$$\frac{\partial C}{\partial t} + \rho \frac{\partial S}{\partial t} = - \frac{\partial C}{\partial x} - \mu_w C \quad [28a]$$

$$-\infty < x < \infty, \quad 0 < t < \infty$$

$$\frac{\partial S}{\partial t} = \kappa(C - S) - \mu_s S \quad [28b]$$

and initial conditions

$$\begin{aligned} C(x, 0) &= f(x) \\ S(x, 0) &= g(x) \end{aligned} \quad -\infty < x < \infty$$

The dimensionless constants in the above equations are given by

$$\rho = \rho^* K_{sw}^* / \theta^*,$$

$$\kappa = \kappa^* L^* / V_w^*,$$

$$\mu_w = (L^* / V_w^*) \mu_w^*, \text{ and}$$

$$\mu_s = (L^* / V_w^*) \mu_s^*.$$

Our first step in the analysis of this initial value problem is to introduce a change of dependent variable to simplify the coupling in the system of equations. If we assume that

$$C(x,t) = e^{(\alpha x + \beta t)} U(x,t) \text{ and } S(x,t) = e^{(\alpha x + \beta t)} V(x,t)$$

are solutions, where

$$\alpha = (1-\rho)\kappa + \mu_s - \mu_w \text{ and}$$

$$\beta = -\kappa - \mu_s,$$

then the functions $U(x,t)$ and $V(x,t)$ must be solutions to the initial value problem

$$U_t = -U_x + (\rho\kappa + \mu_s)V$$

$$-\infty < x < \infty, \quad 0 < t < \infty$$

$$V_t = \kappa U$$

with initial conditions

$$U(x,0) = e^{-\alpha x} f(x)$$

and

$$V(x,0) = e^{-\alpha x} g(x).$$

As in the original problem, this is a system of hyperbolic partial differential equations with constant coefficients. If we choose as a new set of independent variables $\xi = x-t$ and $\eta = x$ in the direction of the characteristics of the system, we obtain a system in canonical form

$$U_\eta = (\rho\kappa + \mu_s)V$$

$$-\infty < \eta < \infty, \quad -\infty < \xi < \eta$$

$$V_\xi = \kappa$$

For this system of equations, the initial conditions transform into the Cauchy conditions

$$U(\eta,\eta) = e^{-\alpha\eta} f(\eta). \text{ and}$$

$$V(\eta,\eta) = e^{-\alpha\eta} g(\eta).$$

If we now differentiate the first equation with respect to ξ and the second

equation with respect to η , we obtain a single second order hyperbolic equation in canonical form

$$U_{\xi\eta} + \lambda^2 U = 0$$

where $\lambda^2 = \kappa(\rho\kappa + \mu_s)$ and the Cauchy conditions can be written

$$U(\eta, \eta) = e^{-\alpha\eta} f(\eta), \text{ and}$$

$$V(\eta, \eta) = \frac{\rho\kappa}{\theta_w V_w} e^{-\alpha\eta} g(\eta).$$

This equation is a version of the telegraph equation. With the problem written in this form, we can apply the theorem on page 124 of Lieberstein (1972) to obtain the following integral representation of the solution in canonical coordinates.

$$U(\xi, \eta) = e^{-\alpha\xi} f(\xi) +$$

$$\int_{\xi}^{\eta} e^{-\alpha y} \left\{ (\rho\kappa + \mu_s) I_0(2\lambda h(y; \xi, \eta)) g(y) + 2\lambda^2 (\eta - y) \frac{I_1(2\lambda h(y; \xi, \eta))}{2\lambda h(y; \xi, \eta)} f(y) \right\} dy \quad [29]$$

$$V(\xi, \eta) = e^{-\alpha\eta} g(\eta) +$$

$$\int_{\xi}^{\eta} e^{-\alpha y} \left\{ \kappa I_0(2\lambda h(y; \xi, \eta)) f(y) + 2\lambda^2 (y - \xi) \frac{I_1(2\lambda h(y; \xi, \eta))}{2\lambda h(y; \xi, \eta)} g(y) \right\} dy \quad [30]$$

where $h(y; \xi, \eta) = \sqrt{(\eta - y)(y - \xi)}$.

Upon substituting $\xi = x - t$, $\eta = x$ and multiplying the result by $\exp(\alpha x + \beta t)$, we have established the following integral representation theorem.

Theorem If $f, g \in C^1(-\infty, \infty)$ and C and S are the unique functions such that $C, C_t, C_x, S, S_t, S_x \in C((-\infty, \infty) \times (0, \infty))$ defined by

$$\frac{\partial C}{\partial t} + \rho \frac{\partial S}{\partial t} = - \frac{\partial C}{\partial x} \quad \mu_w C$$

$$-\infty < x < \infty, \quad 0 < t < \infty$$

$$\frac{\partial S}{\partial t} = \kappa(C - S) \quad \mu_s S$$

and

$$C(x,0) = f(x)$$

$$-\infty < x < \infty$$

$$S(x,0) = g(x)$$

then, for each $(x,t) \in (-\infty, \infty) \times (0, \infty)$,

$$C(x,t) = e^{(\alpha+\beta)t} f(x-t) + \int_{x-t}^x \left\{ (\rho\kappa + \mu_s) I_0(2\lambda\sqrt{(x-y)(y-x+t)}) g(y) + 2\lambda^2(x-y) \frac{I_1(2\lambda\sqrt{(x-y)(y-x+t)})}{(2\lambda\sqrt{(x-y)(y-x+t)})} f(y) \right\} e^{\alpha(x-y)+\beta t} dy \quad [31a]$$

$$S(x,t) = e^{\beta t} g(x) + \int_{x-t}^x \left\{ k I_0(2\lambda\sqrt{(x-y)(y-x+t)}) f(y) + 2\lambda^2(y-x+t) \frac{I_1(2\lambda\sqrt{(x-y)(y-x+t)})}{(2\lambda\sqrt{(x-y)(y-x+t)})} g(y) \right\} e^{\alpha(x-y)+\beta t} dy \quad [31b]$$

We note here, that if f and g are not in C^1 , as is the case for the plug problem, then the above integral representation gives the weak solution to the problem.

The above analytical solution was programmed in FORTRAN 77 for implementation on the VAX 8650 computer at USU. The FORTRAN version was constructed so as to accept input data files that are identical to those used in the VIP numerical model described above, to ensure that the comparisons were made using identical model parameters. The use of the analytical solution for evaluating the VIP model is now described.

Accuracy of Numerical Model Calculations

For the first set of comparisons, a series of simulations were carried out using the numerical VIP model and the analytical solution, for the simplified case described above. Three different sets of initial conditions and five values of the mass transfer parameter, κ , were used. Model input for the first two sets of simulations is given in Table 12 and for the last set of simulations is given in Table 13. Table 14 contains the descriptions of variables used, units and data sources. Both models were simulated for 12 days, and the accuracy comparisons were based on 1) visual inspection of the concentration vs. depth profiles for both the aqueous and soil phases, and 2) comparison of the relative difference between the solutions at the peak concentrations as a function of the mass transfer rate parameter, κ . Figures 27 to 29 demonstrate the comparisons of the depth profiles calculated by the analytical solution to numerical solution

Table 12. Model input values for the first two sets of analyses.

CO	SO				
RHO	PHI	SHC	SMLB		
XMUC	XMUS	KSW	VWPRIME	RWS	
TIMMAX	TOUT	DZ	NZOUT	NPLOW	NTREAT
2000	0.00521				
1.38E6	0.40	1.0	4.90		
0.0	0.0	2.5E-6	0.043	100	
12	6	0.015	2	12	74
2000	0.00521				
1.38E6	0.40	1.0	4.90		
0.0	0.0	2.5E-6	0.043	1.0	
12	6	0.015	2	12	74
2000	0.00521				
1.38E6	0.40	1.0	4.90		
0.0	0.0	2.5E-6	0.043	0.1	
12	6	0.015	2	12	74
2000	0.00521				
1.38E6	0.40	1.0	4.90		
0.0	0.0	2.5E-6	0.043	0.01	
12	6	0.015	2	12	74
2000	0.00521				
1.38E6	0.40	1.0	4.90		
0.0	0.0	2.5E-6	0.043	0.0	
12	6	0.015	2	12	74

(VIP model) with constituent initially in the water, soil and both phases.

Table 13. Model input values for the last set of analyses.

CO	SO				
RHO	PHI	SHC	SMLB		
XMUC	XMUS	KSW	VWPRIME	RWS	
TIMMAX	TOUT	DZ	NZOUT	NPLOW	NTREAT
22984	0.00521				
1.38E6	0.40	1.0	4.90		
0.0	0.0	2.5E-6	0.043	100	
120	10	0.015	2	15	74
22984	0.00521				
1.38E6	0.40	1.0	4.90		
0.0	0.0	2.5E-6	0.043	1.0	
120	10	0.015	2	15	74
22984	0.00521				
1.38E6	0.40	1.0	4.90		
0.0	0.0	2.5E-6	0.043	0.1	
120	5	0.015	2	15	74
22984	0.00521				
1.38E6	0.40	1.0	4.90		
0.0	0.0	2.5E-6	0.043	0.01	
120	1	0.015	2	15	74
22984	0.00521				
1.38E6	0.40	1.0	4.90		
0.0	0.0	2.5E-6	0.043	0.0	
120	1	0.015	2	15	74

Table 14. Descriptions of variables used, units, and data sources.

CO, SO = the initial constituent concentration in water (g/m^3) and in soil (g/g -soil) phase. The initial constituent concentration was set to one of the three initial conditions: initially only in water phase, initially only in soil phase, and initially in both water and soil phase.

RHO = bulk density (g/m^3). This value was chosen from the work of Grenney et al. (1987).

PHI = soil porosity (m^3/m^3), volume of void space/total volume. This value was chosen from the work of Grenney et al. (1987).

SHC = saturated hydraulic conductivity, m/day , the default value of 1.0 as used in the EPA Land Treatment Manual was used in this case.

SMLB = soil moisture coefficient. This value was taken from Clapp and Hornberger (1978).

XMUC, XMUS = first order decay rate for the constituent within the water phase and soil phase, (day^{-1}). All have been set to zero since no constituent decay assumed in either water phase or soil phase.

KSW = soil/water partition coefficient, $(\text{g}/\text{g}\text{-soil})/(\text{g}/\text{m}^3\text{-water})$. The soil/water partition coefficient was derived from Grenney et al. (1987).

VWPRIME = average recharge rate, $(\text{m}^3/\text{day})/\text{m}^2$. This value was chosen from the work of Grenney et al. (1987) using naphthalene under high flow rate condition.

RWS = mass transfer rate coefficient, (day^{-1}). This parameter controls the dispersion on concentration with depth curves and breakthrough curves. A range of 100, 1, 0.1, 0.01, 0, was used to demonstrate the curve changes with it.

TIMMAX = the length of run, days. 12 days and 120 days were used for concentration with depth and breakthrough curves analyses, respectively.

TOUT = the time for output, days.

DZ = the depth increment, m. 0.015 was used in this study.

NZOUT = number of depth increment for output file. 2 was used to make 0.03m depth increment for output file.

NPLOW = number of depth increment for plow zone. 15 was used to make 0.15m depth of plow zone.

NTREAT = number of depth increment for treatment zone.

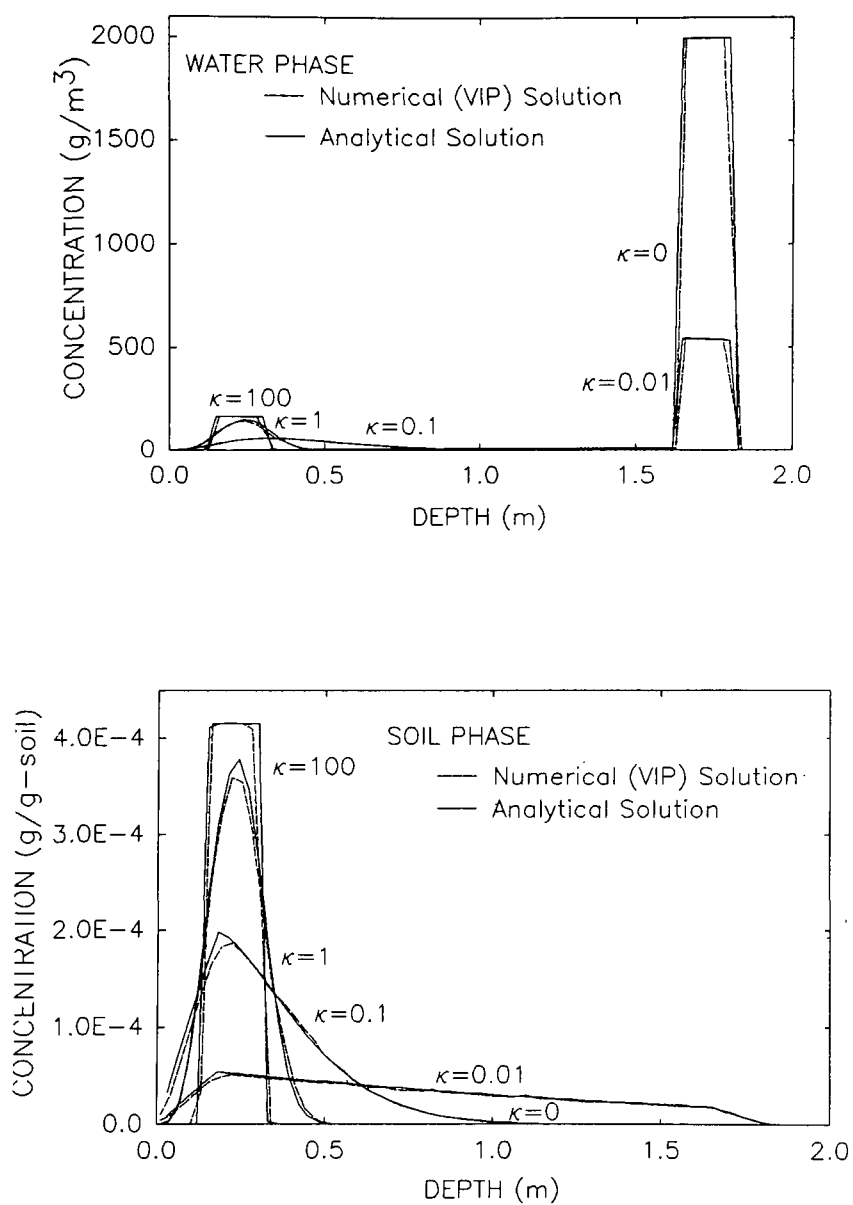


Figure 27. Comparison of the depth profiles calculated by the analytical solution to the numerical solution (VIP model) with constituent initially in the water phase.

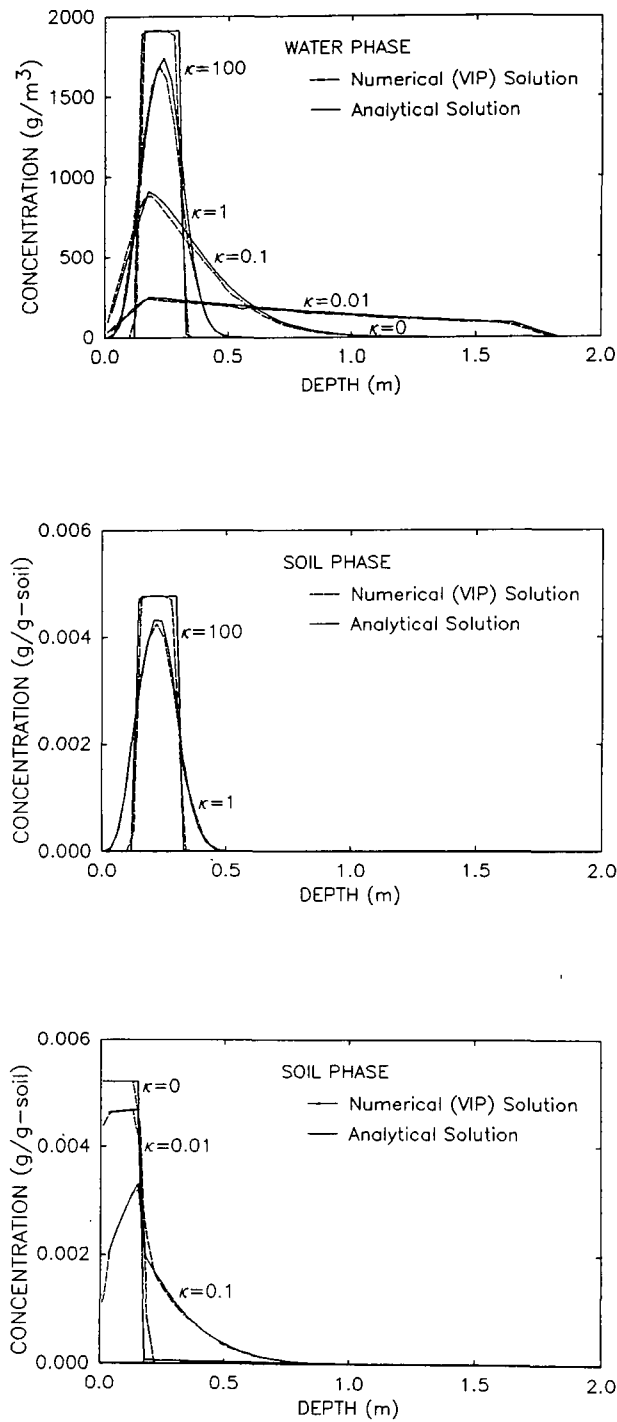


Figure 28. Comparison of the depth profiles calculated by the analytical solution to the numerical solution (VIP model) with constituent initially in the soil phase.

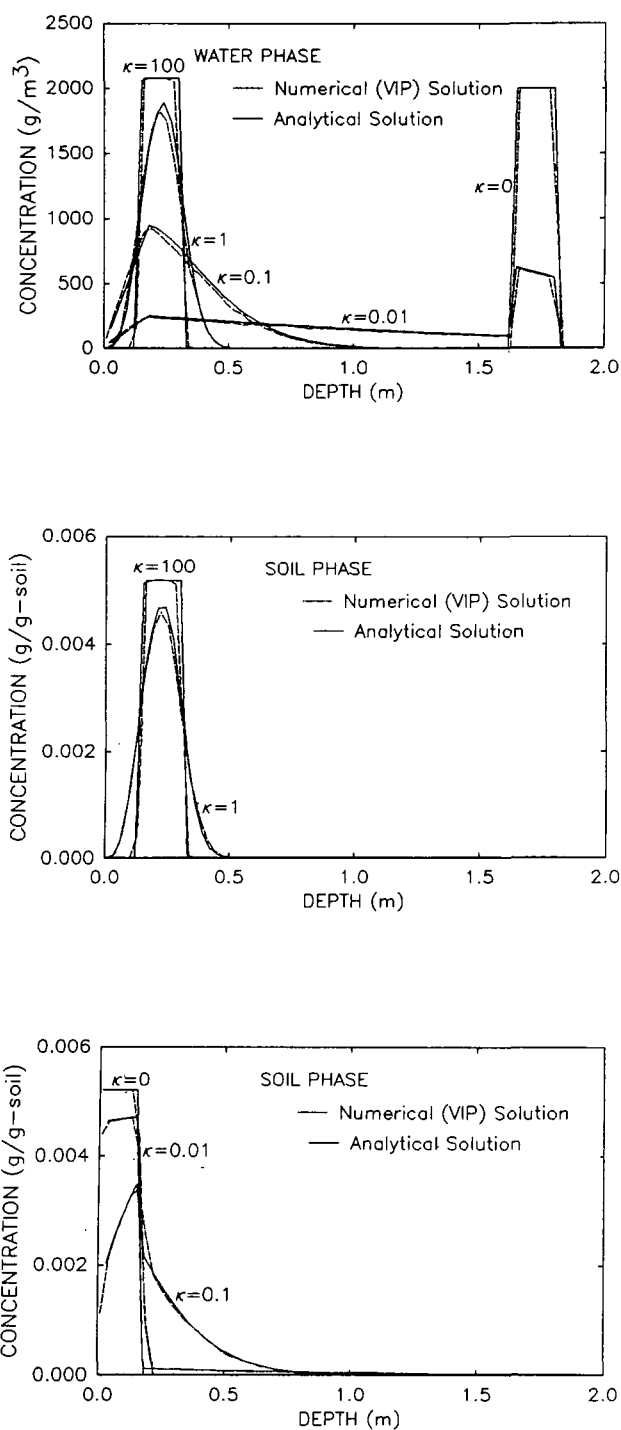


Figure 29. Comparison of the depth profiles calculated by the analytical solution to the numerical solution (VIP model) with constituent initially in both phases.

Comparing the depth profiles from the numerical solution and the analytical solution for five different mass transfer rate coefficients in either the water phase or the soil phase, there is little visible difference. Figures 30 and 31 present the percent relative error between the results from numerical VIP solution and analytical solution vs. the mass transfer rate coefficient κK in the water phase and the soil phase, respectively. Table 15 lists the definition of the percent relative error and appropriate notation. The relative errors in both the soil phase and water phase are less than 7 percent over the entire range of κ investigated. Thus, the numerical solution in the VIP model accurately represented the nonequilibrium sorption/desorption kinetics for the wide range of mass transfer rate coefficients ($0 \leq \kappa \leq 1000$) considered.

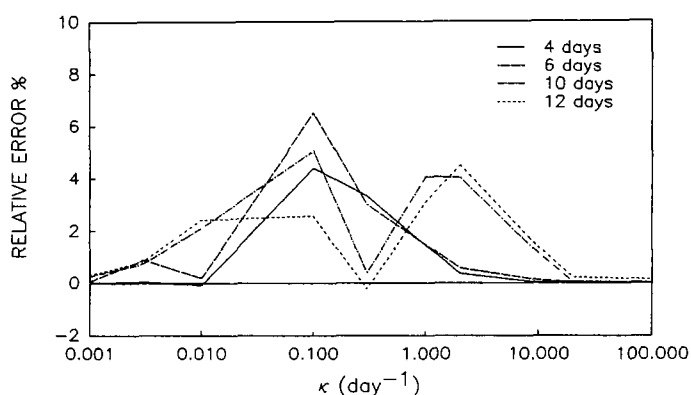


Figure 30. Relative error % vs κ in the water phase.

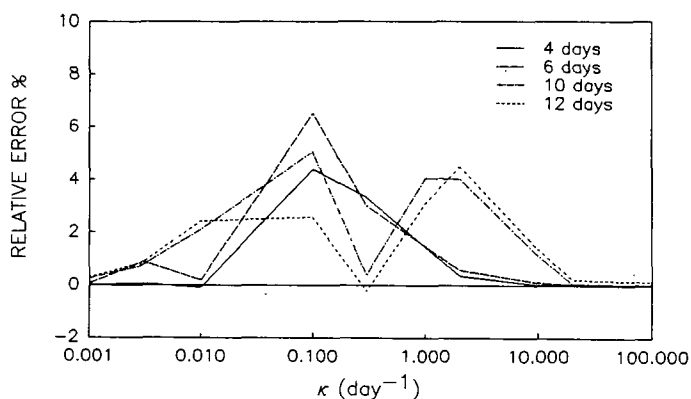


Figure 31. Relative error % vs κ in the soil phase.

Table 15. The definition of the percent relative error and notation.

Definition of Percent Relative Error	
Water Phase	$100 (C_a - C_n) / C_a$
Soil Phase	$100 (S_a - S_n) / S_a$
Definition of the Notation	
Water Phase:	
C_a : Peak concentration in water phase by analytical solution	
C_n : Peak concentration in water phase by numerical (VIP) solution	
Soil Phase:	
S_a : Concentration in soil phase by analytical solution	
S_n : Concentration in soil phase by numerical (VIP) solution	

Experimental verification of the VIP model was recently provided by Reinhart (1988) who studied the transport and fate of eleven organic compounds, including halogenated aliphatic, chlorinated phenols and benzenes, pesticides, and PNAs, in laboratory columns packed with municipal refuse. The VIP model was fit to experimental data for depth profiles and breakthrough curves by adjusting the solid-liquid mass transfer rate coefficients and partition coefficients. Based on this procedure, close agreement between the model and the data were found, and the best fit values of K_{sw} agreed well with those found from independent equilibrium tests. These results will be published in early 1989.

EFFECT OF MASS TRANSFER COEFFICIENT ON MODEL BEHAVIOR

Concentration Distribution Curves

Figure 27 shows the concentration distribution curves in the water and soil phases after 12 days with the concentration initially in water phase only. For κ equals zero, that is, for no exchange between the water and soil phases, all of the constituent concentration moves with the water phase at the pore water velocity, and the constituent concentration in the soil phase is zero because there is no initial mass in the soil phase. When κ increases in value, that is, when the speed of exchange between water and soil phases increases, the amplitude of the concentration in water phase decreases, the constituent concentration releases from the water phase to the soil phase so that there is a long tail formed for soil phase profile ($\kappa = 0.01$). When κ increases further, the amplitude of the concentration in the water phase decreases rapidly and the profile becomes retarded and dispersive, and the amplitude of the concentration in the soil phase increases but is asymmetric ($\kappa = 0.1$).

As the water phase peak moves sufficiently down in the soil column, the algebraic sign on $dS/dt = \kappa(K_{sw}C - S)$ changes from + to -, thereby changing this term in the soil phase transport model from a "sink" to a "source". When κ becomes very large ($\kappa = 100$), the exchange between the water and the soil phases becomes very fast, the peak concentration in soil and water phases are 0.000415 g-const./g-soil and 166.27 g-const./m³-water respectively, and the instantaneous partition coefficient is $0.000415/166.27 = 2.496 \times 10^{-6}$ (g/g-soil)/(g/m³-water), which is very close to the equilibrium partition coefficient 2.5×10^{-6} (g/g-soil)/(g/m³-water).

The results for the case with the initial mass in the soil phase demonstrated in Figure 28 is similar to the results with the initial concentration in the water phase.

The behavior of the water and soil phase profiles shown in Figure 29 shows the effects of the parameter κ which is the measure of the speed of exchange between the two phases. For κ equals zero, that is, for no exchange between the water and soil phase, the curves show that both phases' distribution profiles tend to be rectangular, the water phase moves due to the pore water velocity and the soil phase does not move: all of the constituent concentration remains in the plow zone. As κ increases in value, that is, when the speed of exchange increases, the amplitude of the concentration decreases, the dispersion of the distribution increases, and the profile after attaining their peaks begin to develop long tails ($\kappa = 1$). As κ increases further, the concentration distribution becomes more dispersed, the original peak of the water phase decreases, the profile becomes more asymmetric and retarded, the considerable tails occur, and the resulting concentration at the tailing end in water phase is higher ($\kappa = 0.1$). As κ becomes very large and the exchange becomes very rapid, the profiles become more nearly symmetrical but move at a retarded velocity (Grenney et al., 1987). When κ approaches ∞ , the concentration distributions tend to be rectangular and retarded: the sorption/desorption processes are fast with respect to the bulk fluid flow rate and "local equilibrium" can be assumed.

Superposition

Figure 27 and Figure 28 show the concentration profiles in the water and soil phases with constituent concentration initially in the water phase and soil phase respectively. If the curves for the water phase (or the soil phase) in Figure 27 and Figure 28 are added together, curves for the water phase (or the soil phase) in Figure 29 can be obtained. Therefore, the concentration profiles with initial concentration in two phases can be obtained by adding the concentration profiles with initial concentration in each phase together either for the analytical solution or the numerical solution.

Breakthrough Curves

Three initial conditions were used: 22984 g/m³ only in the water phase; 0.00521 g/g-soil only in the soil phase; 22984 g/m³ in the water phase with 0.00521 g/g-soil in the soil phase. The numerical solution of the VIP model was used to investigate the breakthrough curves at a depth of 1.0 meter, for different mass transfer rate coefficients (κ) in the range from 0 to 100 per day, with these three initial conditions.

Figure 32 presents the breakthrough curves for the initial concentration of the water phase only, while Figure 33 shows the breakthrough curves with the concentration initially only in the soil phase. Figure 34 demonstrates the breakthrough curves for the initial concentration in both the water and soil phases. When κ equals zero, there is no exchange between the two phases, the concentration profile in the water phase is a narrow rectangle without dispersion, and there is no concentration in the soil phase at the point of 1.00 depth. When κ is small, a slow exchange of material between two phases takes place, causing a significant decrease in the peak concentration and a considerable tailing in the water phase profile, and a flat low amplitude peak profile in the soil phase is formed ($\kappa = 0.01$).

With increasing values of the mass transfer coefficient, a broad low amplitude peak of the water profile is formed and the concentration at the tailing end of the water profile is higher, the concentration amplitude of the soil profile is getting higher, and both of the profiles become symmetrical in shape and exhibit dispersion ($\kappa = 0.1$). As κ approaches ∞ , the profile of the water phase tends to be rectangular again, but maintain a wider and lower amplitude peak than when κ equals zero. The profile of the soil phase also tends to be rectangular, but shows a significant increase in the peak concentration.

Dispersion Due to κ

The curves in Figure 32 and Figure 33 demonstrate that for intermediate values of κ ($0.1 < \kappa < \infty$), the calculated breakthrough curve shows a pronounced dispersive tendency, even though the model Equations [1a] and [1b] do not contain an explicit hydrodynamic dispersion term, $D_e(\partial^2 C / \partial x^2)$. Further, the close agreement between the analytical solution and the numerical VIP solution shown in Figure 27 through 29 precludes the possibility of numerical dispersion, common in many finite difference approximations of the convection term in Equation [1a]. This clearly demonstrates that it is possible to observe apparent "dispersion" in solute transport in a sorbing environment in the absence of hydrodynamic dispersion. These results are pertinent in unsaturated flow regimes in which such hydrodynamic dispersion is not probable. These results are similar to those observed by Stevens et al. (1986) with two-phase mass transfer effects in biofilm processes.

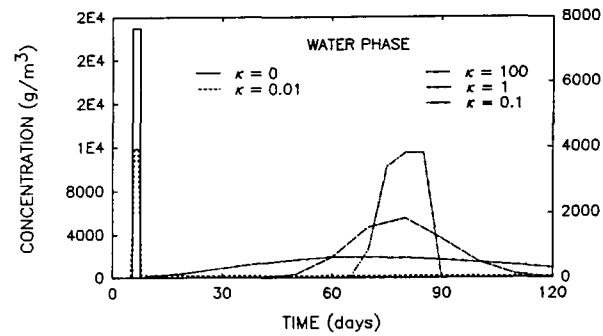


Figure 32. Breakthrough curve predicted by the VIP model with the initial concentration in the water phase.

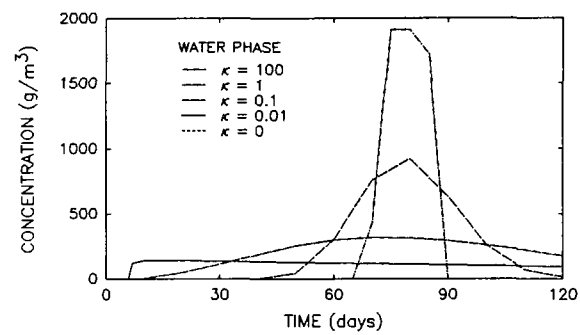


Figure 33. Breakthrough curve predicted by the VIP model with the initial concentration in the soil phase.

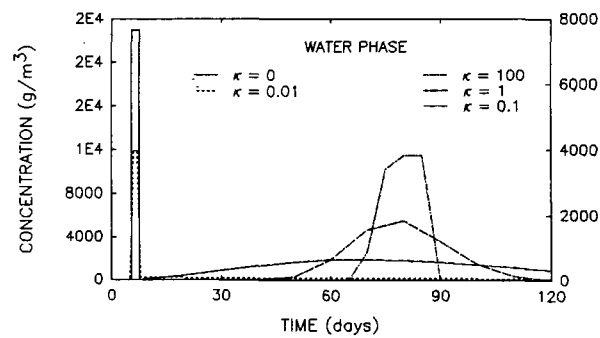


Figure 34. Breakthrough curve predicted by the VIP model with the initial concentration in both phases.

Estimation of κ from VIP Model

Figures 32 through 34 demonstrate that the calculated breakthrough curves from the VIP model vary with κ values. Once a breakthrough curve from field data is obtained and compared on the same graph with a group of different values of κ , there should be one curve for a specific value of κ which is in close agreement to the field data within a certain level of confidence. This can be estimated by "curve-fitting" the model to the measured data (van Genuchten and Wierenga, 1977; van Genuchten et al., 1977; Gaudet et al., 1977; Rao et al., 1979; Rao et al., 1980a; Rao et al., 1980b). These techniques were discussed by Rao et al. (1979). The VIP model provides a methodology by which estimates of κ may be obtained, similar to that described by Liu and Weber (1981) for estimating film diffusion coefficients in activated carbon adsorption columns. Since relatively little is known about the factor κ or the functional form which κ follows, this technique can provide a means to estimate κ under different experimental conditions for analysis of the effects of those conditions on κ . This will lead to improved understanding of hazardous waste constituent interactions in the vadose zone.

REFERENCES

- Baehr, A. and M. Y. Corapcioglu. 1984. Predictive model for pollution from gasoline in soils and ground water, paper presented at Proceedings, NWWA Conference-Petroleum Hydrocarbons and Organic Chemicals in Ground Water, Natl. Water Well Assoc. Houston, Tex.
- Bella, D.A. and W.J. Grenney. 1970. Finite-difference Convection Errors. J. of San. Engr. Div., ASCE. 96(SA6):1361-1375.
- Borden, D. R. and P. B. Bedient. 1986. Transport of dissolved hydrocarbons influenced by oxygen-limited biodegradation 1. Theoretical Development. Water Resour. Res. 22(13):1973-1982.
- Bossert, I., Kachel, W.M., and Bartha, R. 1984. Fate of hydrocarbons during oily sludge disposal in soil. Appl. and Environ. Microbiol. 47:763-767.
- Brady, N.C. 1974. The nature and properties of soils. Eighth edition. Macmillan Publishing Co. Inc. New York, NY.
- Cameron, D. A. and A. Klute. 1977. Convective-dispersive solute transport with a combined equilibrium and kinetic adsorption model. Water Resour. Res. 13(1):183-188.
- Caupp, C. L., W. J. Grenney, P. J. Ludvigsen. 1987. VIP Manual: A model for the evaluation of hazardous substances in the soil. Department of Civil and Environmental Engineering, Utah State University, Logan, Utah 84322-4110.
- Clapp, R. B. and G. Hornberger. 1978. Empirical equations for some soil hydraulic properties. Water Resour. Res. 14:601-604.
- Coats, K. H., and B. D. Smith, 1964. Dead-end pore volume and dispersion in porous media. Soc. Pet. Eng. J. 4:73-84.
- Coover, M.P. 1987. Studies of the persistence of polycyclic aromatic hydrocarbons in two unacclimated agricultural soils. Thesis. Department of Civil and Environmental Engineering. Utah State University. Logan, Utah.
- Coover, M.P., R.C. Sims, and W.D. Doucette. 1987. Extraction of polycyclic aromatic hydrocarbons from spiked soil. J. of the Assoc. of Official Analytical Chemists. 70:1018-1020.
- Davidson, J. M., P. S. C. Rao, R. E. Green, and H. D. Selim. 1980. Evaluation of conceptual models for solute behavior in soil-water systems. In A. Banin and U. Kafkafi (Eds.). Agrochemicals in soils. Proc. of Inter-congress of ISSS held at Jerusalem, Israel. June 1976. Pergamon Press, London.
- De Camargo, O. A., J. W. Giggar, and D. R. Nielsen. 1979. Transport of inorganic phosphorus in an alfisol. Soil Sci. Soc. Am. J. 43(5):884-890.

Dibble, J.T. and R. Bartha. 1979. Effect of environmental parameters on the biodegradation of oil sludge. *Appl. and Environ. Microbiol.* 37:729.

Enfield, C.G., R.F. Carsel, S.Z. Cohen, T. Phan, and D.M. Walters. 1982. Approximating pollutant transport in ground water. *Groundwater*. 20:(6)711-722.

Enfield, C. G., D. M. Walters, J. T. Wilson, and M. D. Piwoni. 1986. Behavior of organic pollutants during rapid-infiltration of wastewater into soil: II Mathematical description of transport and transportation. *Hazardous Waste and Hazardous Materials*. 3(1):57-76.

Federal Register. 1982. Hazardous waste management system: Requirements for land disposal facilities.

Fava, A. and H. Eyring. 1956. Equilibrium and kinetics of detergent adsorption: A generalized equilibration theory. *J. Phys. Chem.* 60:890-898.

Gaudet, J. P., J. Jegat, G. Vachaud, and P. J. Wierenga. 1977. Solute transfer with exchange between mobile and stagnant water, through unsaturated sand. *Soil Sci. Soc. Am. J.* 41:665-671.

Goldstein, S. 1953a. On the mathematics of exchange processes in fixed columns: I. Mathematical solutions and asymptotic expansions. *Proc. Roy. Soc. London Ser. A*, 219:151-171.

Goldstein, S. 1953b. On the mathematics of exchange processes in fixed columns: II. The equilibrium theory as the limit of the kinetic theory. *Proc. Roy. Soc. London Ser. A*, 219:171-185.

Goldstein, S. 1959a. On the mathematics of exchange processes in fixed columns: III. The solution for general entry conditions. *Proc. Roy. Soc. London Ser. A*, 252:334-347.

Goldstein, S. 1959b. On the mathematics of exchange processes in fixed columns: IV. Limiting values, and correction terms, for kinetic theory solutions with general entry conditions. *Proc. Roy. Soc. London Ser. A*, 252:348-359.

Goldstein, S. 1959c. On the mathematics of exchange processes in fixed columns: V. The equilibrium theory and perturbation solutions, and their connection with kinetic theory solutions, for general entry conditions. *Proc. Soc. London Ser. A*, 252:360-375.

Goltz, M.N., and P.V. Roberts. 1986. Interpreting organic solute transport data from a field experiment using physical nonequilibrium models. *J. of Contaminant Hydrology*. 1:77-93.

Gray, T.R.G. 1981. Microbiological aspects of the soil, plant, air, and animal environments: The soil and plant environments. p.19-38. *In* I.R. Hill and S.J.L. Wright (Eds.). *Pesticide Microbiology*. Academic Press, New York, NY.

- Grenney, W. J., C. L. Caupp, R. C. Sims and T. E. Short. 1987. A mathematical model for the fate of hazardous substances in soil: Model description and experimental results. *Haz. Wastes and Haz. Mat.* 4(3):223-239.
- Grenney, W.J., M.C. Teuscher, and L.S. Dixon. 1978. Characteristics of the Solution algorithms for the QUAL II river model. *J of the Wat. Poll. Cont. Fed.* 50(1):151-157.
- Grenney, W.J., R.C. Thompson, Z. Yan and D.K. Stevens. Dispersion in the vadose zone due to nonequilibrium adsorption kinetics, Department of Civil and Environmental Engineering, Utah State University, Logan, Utah 84322 (Submitted for review).
- Hamaker, J.W. 1972. Organic chemicals in the soil environment. Vol. 1, Goring. p. 253. C.A.I. and Hamaker, J.W., Marcel Dekker, Inc. New York.
- Hann, R.W., Jr., and P.J. Young. 1972. Mathematical models of water quality parameters for rivers and estuaries, p.424. Texas Water Resources Institute Report TR-45. Texas A & M University.
- Harleman, D.R.F., C.H. Lee, and L.C. Hall. 1968. Numerical studies of unsteady dispersion in estuaries. *J. of the San. Engr. Div., ASCE.* 94:(SA5)897-911.
- Harris, R.F. 1981. Effect of water potential on microbial growth and activity. p.23-95. In: Water potential relations in soil microbiology. SSSA special publication number 9. Soil Sci. Soc. Am., Madison, WI.
- Hashimoto, I., K. B. Deshpande and H. C. Thomas. 1964. Peclet numbers and retardation factors for ion exchange columns. *Ind. and Eng. Chem. Fund.* 3:213-218.
- Herbes, S.E. 1981. Rates of microbial transformation of polycyclic aromatic hydrocarbons in water and sediments in the vicinity of a coal-coking wastewater discharge. *Appl. and Environ. Microbiol.* 41:20-28.
- Herbes, S.E., and Schwall, L.R. 1978. Microbial transformations of polycyclic aromatic hydrocarbon in pristine and petroleum-contaminated sediments. *Appl. and Environ. Microbiol.* 35:306.
- Holley, E.R., Jr. and D.R.F. Harleman. 1965. Dispersion of pollutants in estuary type flows, hydrodynamics laboratory, p.191. Report No. 74. MIT, Cambridge 39, Massachusetts.
- Hornsby, A. G. and J. M. Davidson. 1973. Solution and adsorbed fluometuron concentration distribution in a water-saturated soil: Experimental and predicted evaluation. *Soil Sci. Soc. Amer. Proc.* 37:823-828.
- Hoffman, D. L., and D. E. Rolston. 1980. Transport of organic phosphate in soil as affected by soil type. *Soil Sci. Soc. Am. J.* 44(1):46-52.
- Jury, W.A., W.F. Spencer, and W.J. Farmer. 1983. Behavior assessment model for trace organics in soil: I. Desorption. *J. Environ. Qual.* 12:558-564.

- Karickhoff, S.W., D.S. Brown, and T.A. Scott. 1979. Sorption of hydrophilic pollutants on natural sediments. *Water Res.* 13:241-248.
- Kay, B. D. and D. E. Elrick. 1967. Adsorption and movement of lindane in soils. *Soil Sci.* 104:314-322.
- Lapidus, L., and N. R. Amundson. 1952. Mathematics of adsorption in beds. VI. The effects of longitudinal diffusion in ion exchange and chromatographic columns. *J. Phys. Chem.* 56:984-988.
- Lieberstein, H. M. 1972. *Theory of partial differential equations.* Academic Press, New York.
- Lindstrom, F. T. and L. Boersma. 1971. A theory on the mass transport of previously distributed chemicals in a water saturated sorbing porous medium. *Soil Sci.* 111:192-199.
- Lindstrom, F. T., L. Boersma, and D. Stockard. 1971. A theory on the mass transport of previously distributed chemicals in a water saturated sorbing porous medium: Isothermal cases. *Soil Sci.* 112:291-300.
- Lindstrom, F. T. and M. N. L. Narasinhham. 1973. Mathematical theory of a kinetic model for dispersion of previously distributed chemicals in a sorbing porous medium. *SIAM J. Appl. Math.* 24:496-510.
- Liu, K.T., J. Walter and Jr. Weber. 1981. Characterization of mass transfer parameters for adsorber modeling and design. *J. Wat. Poll. Cont. Fed.* 53:1541-1549.
- Loehr, R.C., 1986. Land treatment: A waste management alternative, p.151. In Loehr, R.C. and Malina, J.F. (Eds.). *University of Texas Center for Research in Water Resources*, Austin, Texas.
- Lyman, W.J., W.F. Rechl and D.H. Rosenblatt. 1982. *Chemical property estimation methods*, McGraw-Hill, New York.
- Mahmood, R. and R.C. Sims. 1986. Mobility of organics in land treatment systems. *Jour. of Environ. Engr.* 112(2):236-245.
- McKenna, E.J. 1977. Biodegradation of polynuclear aromatic hydrocarbon pollutants by soil and water microorganisms. Presented at the 70th annual meeting of the American Institute of Chemical Engineers. Nov. 13-17. New York.
- McLean, J.E., R.C. Sims, W.J. Doucette, C.R. Caupp, and W.J. Grenney. 1988. Evaluation of mobility of pesticides in soil using U.S.EPA methodology. *J. Environ. Engr. Div., ASCE.* 114:689-703.
- Mears, D.E. 1971. The role of axial dispersion in trickle-flow laboratory reactors. *Chem. Engr. Sci.* 26:1361-1366.

Metcalf and Eddy Inc. 1979. Wastewater engineering: Treatment disposal, reuse. 2nd Edition. McGraw-Hill, New York, NY. 782 p.

Molz, F. J., M. A. Widdowson, and L. D. Benefield. 1986. Simulation of microbial growth dynamics coupled to nutrient and oxygen transport in porous media. *Water Resour. Res.* 22(8):1207-1216.

Nielsen, D. R., and J. W. Biggar. 1961. Miscible displacement in soils, 1 Experimental information. *Soil Sci. Soc. Am. Proc.* 25(1):1-5.

Nielsen, D. R., M. Th. van Genuchten and J. W. Giggarr. 1986. Water flow and solute transport processes in the unsaturated zone. *Water Resour. Res.* 22:89S-108S.

Nkedi-Kizza, P., J. W. Biggar, H. M. Selim, M. Th. van Genuchten, P. J. Wierenga, J. M. Davidson, and D. R. Nielsen. 1984. On the equivalence of two conceptual models for describing ion exchange during transport through an aggregated oxisol. *Water Resour. Res.*, 20(8):1123-1130.

O'Connor, D.J., J.P. St. John, and D.M. DiToro. 1968. Water quality analysis of the Delaware River estuary. *Journal of the San. Engr. Div., ASCE.* 94:(SA6)1225-1252.

Parker, L.W. and K.G. Doxtader. 1983. Kinetics of the microbial degradation of 2,4-D in soil: Effects of temperature and moisture. *J. Environ. Qual.* 12:553.

Passioura, J.B. 1971. Hydrodynamic dispersion in aggregated media. *Soil Sci.* 11:339-344.

PACCE (Petroleum Association for Conservation of the Canadian Environment). 1985. The persistence of polynuclear aromatic hydrocarbons in soil. Report No. 85-2. Ottawa, Ontario.

Petersen, E.E. 1963. Chemical reaction analysis. Prentice-Hall, Inc. Englewood Cliffs, New Jersey.

Philip, J. R. 1968. Diffusion, dead-end pores and linearized absorption in aggregated media, *Aust. J. Soil Res.* 6:21-30.

Prych, E.A., and T.R.E. Chidley. 1969. Discussion on numerical studies of unsteady dispersion in estuaries. *J. of the San. Engr. Div., ASCE.* 95:(SA5)959-967.

Rao, P. S. C., J. M. Davidson, and H. M. Selim. 1979. Evaluation of conceptual models for describing nonequilibrium adsorption-desorption of pesticides during steady flow in soils, *Soil Sci. Soc. Am. J.* 43(1):22-28.

Rao, P. S. C., and R. E. Jessup. 1983. Sorption and movement of pesticides and other toxic organic substances in soils, p. 183-201. In D. W. Nelson, D. E. Elrick, and K. K. Tanji (Eds.). *Chemical Mobility and Reactivity in Soil Systems*, Soil Science Society of America, Madison, Wisc.

- Rao, P. S. C., R. E. Jessup, D. E. Rolston, J. M. Davidson, and D. P. Kilcrease. 1980a. Experimental and mathematical description of nonadsorbed solute transfer by diffusion in spherical aggregates. *Soil Sci. Soc. Am. J.* 44:684-688.
- Rao, P. S. C., D. E. Rolston, R. E. Jessup, and J. M. Davidson. 1980b. Solute transport in aggregated porous media: Theoretical and experimental evaluation. *Soil Sci. Soc. Am. J.* 44:1139-1146.
- Reinhart, R.D. 1988. Personnel communication.
- Ryan, J., Loehr, R. and Sims, R. 1987. The land treatability of appendix VIII constituents present in petroleum refinery wastes: Laboratory and modeling studies. Prepared for the American Petroleum Institute.
- Ryan, J. 1986. Land treatment: A waste management alternative. p.347. In Loehr, R.C. and Malina, J.F. (Eds.). University of Texas Center for Research in Water Resources, Austin, Texas.
- Schwarzenbach, R.P., and J. Westall. 1981. Transport of nonpolar organic compounds from surface water to groundwater. *Environmental Science and Technology*. 15(11):1360-1367.
- Selim, H. M., J. M. Davidson, and R. S. Mansell. 1976. Evaluation of a two-site adsorption-desorption model for describing solute transport in soils, paper presented at Proceedings, Summer Computer Simulation Conference, Nat. Sci. Found. Washington, D. C. July 12-14.
- Short, T.E. 1986. Modeling of processes in the unsaturated zone. In Land Treatment: A hazardous waste management alternative, p. 211-240. In R.C. Loehr and J.F. Malina, Jr. (Eds.). Water Resources Symposium No. 13, Center for Research in Water Resources. University of Texas at Austin, Austin, Texas.
- Sims, R.C. and M.R. Overcash. 1983. Fate of polynuclear aromatic compounds (PNAs) in soil-plant systems. *Residue Reviews*. 88:1-68.
- Sims, R.C. 1982. Land treatment of polynuclear aromatic compounds. Ph.D. Dissertation. North Carolina State University. Raleigh, North Carolina.
- Sims, R.C. 1986. Land treatment: A waste management alternative, p.151. In Loehr, R.C. and Malina, J.F. (Eds.). University of Texas Center for Research in Water Resources, Austin, Texas.
- Smith, O.L. 1982. Soil microbiology: A model of decomposition and nutrient cycling, p. 161. In M. J. Bazin (Ed.). CRC Press, Inc., Boca Raton.
- Soil Science Society of America. 1981. Water potential relations in soil microbiology. p.151. SSSA special publication No.9. Soil Science Society of America, Madison, WI.
- Stevens, D. K., P. M. Berthouex and T. W. Chapman. 1986. The effect of tracer diffusion in biofilm on residence time distributions. *Wat. Res.* 20(3):369-375.

Stotzky, G. 1972. Activity ecology and population dynamics of microorganisms in soil. *CRC Critical Reviews in Microbiology* 2:59-137.

Stotzky, G. 1980. Surface interactions between clay minerals and microbes, viruses and soluble organics, and the probable importance of these interactions to the ecology of microbes in soil. p.231-247. In R.C.W. Berkeley, J.M. Lindi, J. Melling, P.R. Rotter, and B. Vincent (Eds.). *Microbial adhesion to surfaces*. John Wiley and Sons, New York, NY.

Symons, B.D., R.C. Sims, and W.J. Grenney. 1988. Fate and transport of organics in soil: Model predictions and experimental results. *J. Wat. Poll. Cont. Fed.*, (in press).

Taylor, J.M, J.F. Parr, L.J. Sikora, and G.B. Willson, 1980. Considerations in the land treatment of hazardous wastes: Principles and practice. In *Proceedings of the Second Oil and Hazardous Materials Spills Conference and Exhibition*, Hazardous Materials Control Research Institute, Silver Springs, MD.

U.S. EPA. 1984 a and b. Review of in-place treatment techniques for contaminated surface soils. Vol 1 and 2. EPA-540/2-84-003 a and b. Hazardous Waste Engineering Research Laboratory, Cincinnati, Ohio.

U.S. EPA. 1986. Permit guidance manual on hazardous waste land treatment demonstrations. Final Draft. EPA-530/SW-032. Prepared for OSW, U.S. Environmental Protection Agency, Washington, D.C.

U.S. EPA. 1986. Waste-soil treatability studies for four complex industrial wastes: methodologies and results. Vol 1 and 2. EPA/600/6-86/003 a and b. Robert S. Kerr Environmental Research Laboratory, Ada, Oklahoma.

U.S. EPA. 1988a. Treatment potential for 56 EPA listed hazardous chemicals in soil. EPA/600/6-88-001. Robert S. Kerr Environmental Research Laboratory, Ada, Oklahoma.

U.S. EPA. 1988b. Interactive simulation of the fate of hazardous chemical during land treatment of oily wastes: RITZ user's guide. EPA/600/8-88-001. Robert S. Kerr Environmental Research Laboratory, Ada, Oklahoma.

Valocchi, A. J., 1985. Validity of the local equilibrium assumption for modeling sorbing solute transport through homogeneous soils, *Water Resour. Res.* 21(6):808-820.

van Genuchten, M. Th., and R. W. Cleary. 1979. Movement of solutes in soil: Computer-simulated and laboratory results, p. 349-386. In G. H. Bolt. Elsevier (Ed.). *Soil Chemistry, Vol. B, Physico-Chemical Models*. New York.

van Genuchten, M. Th., and P. J. Wierenga. 1976. Mass transfer studies in sorbing porous media, I. Analytical solutions, *Soil Sci. Soc. Am. J.* 40(4):473-480.

van Genuchten, M. Th., D. H. Tang and R. Guennelon. 1984. Some exact and approximate solutions for solute transport through large cylindrical macropores. *Water Resour. Res.* 20:335-346.

van Genuchten, M. Th., J. M. Davidson, and P. J. Wierenga. 1974. An evaluation of kinetic and equilibrium equations for the prediction of pesticide movement in porous media. *Soil Sci. Soc. Am. Proc.* 38:29-35.

van Genuchten, M. Th., and P. J. Wierenga. 1977. Mass transfer studies in sorbing porous media: II. Experimental evaluation with tritium ($^3\text{H}_2\text{O}$). *Soil Sci. Soc. Am. J.* 41:272-278.

van Genuchten, M. Th., P. J. Wierenga, and G. A. O'Connor. 1977. Mass transfer studies in sorbing porous media: III. Experimental evaluation with 2,4,5-T. *Soil Sci. Soc. Am. J.* 41:278-285.

Walker, A. 1974. A simulation model for prediction of herbicide persistence. *J. Environ. Qual.* 3:396-401.

Yan, Z. 1988. Evaluation of the vadose zone interactive processes (VIP) model using nonequilibrium adsorption kinetics and modification of VIP model. Thesis. Department of Civil and Environmental Engineering. Utah State University. Logan, Utah.

Appendix A

Nonlinear Least Squares Analysis of Temperature Data

Non-Linear Least Squares Parameter Estimation

Benzo[b]fluoranthene Temperature Data

After 5 iteration(s), converged parameter estimates are

k_{20}	C_0	θ		
.167757E-02 day ⁻¹	.103676E+01	.102365E+01		
X(1) Time	X(2) Temp.	OBS C/C ₀	ETA Predicted	Resid
.0000	10.00	1.150	1.037	.1132
.0000	10.00	1.130	1.037	.9324E-01
.0000	10.00	1.070	1.037	.3324E-01
.0000	20.00	1.180	1.037	.1432
.0000	20.00	1.120	1.037	.8324E-01
.0000	20.00	1.190	1.037	.1532
.0000	30.00	1.260	1.037	.2232
.0000	30.00	1.160	1.037	.1232
.0000	30.00	1.020	1.037	-.1676E-01
10.00	10.00	1.080	1.023	.5691E-01
10.00	10.00	.9700	1.023	-.5309E-01
10.00	10.00	1.030	1.023	.6912E-02
10.00	20.00	.9600	1.020	-.5952E-01
10.00	20.00	.8900	1.020	-.1295
10.00	20.00	1.050	1.020	.3048E-01
10.00	30.00	.9200	1.015	-.9502E-01
10.00	30.00	1.050	1.015	.3498E-01
10.00	30.00	1.020	1.015	.4976E-02
60.00	10.00	.9100	.9574	-.4736E-01
60.00	10.00	.9600	.9574	.2636E-02
60.00	10.00	.9700	.9574	.1264E-01
60.00	20.00	.8800	.9375	-.5749E-01
60.00	20.00	.8900	.9375	-.4749E-01
60.00	20.00	.8800	.9375	-.5749E-01
60.00	30.00	.8100	.9130	-.1030
60.00	30.00	.8300	.9130	-.8297E-01
60.00	30.00	.8400	.9130	-.7297E-01
94.00	10.00	.8000	.9151	-.1151
94.00	10.00	.8100	.9151	-.1051
94.00	10.00	.8300	.9151	-.8510E-01
94.00	20.00	.8200	.8855	-.6551E-01
94.00	20.00	.8100	.8855	-.7551E-01
94.00	20.00	.8200	.8855	-.6551E-01
94.00	30.00	.7800	.8495	-.6950E-01
94.00	30.00	.7600	.8495	-.8950E-01
94.00	30.00	.7600	.8495	-.8950E-01
120.0	10.00	.8800	.8840	-.4044E-02
120.0	10.00	.8900	.8840	.5956E-02
120.0	20.00	.8500	.8477	.2278E-02
120.0	20.00	.8700	.8477	.2228E-01
120.0	20.00	.8900	.8477	.4228E-01
120.0	30.00	.7600	.8040	-.4396E-01
120.0	30.00	.7400	.8040	-.6396E-01

120.0	30.00	.8000	.8040	-.3961E-02
150.0	10.00	.8500	.8495	.4821E-03
150.0	10.00	.8700	.8495	.2048E-01
150.0	10.00	.8700	.8495	.2048E-01
150.0	20.00	.7700	.8061	-.3611E-01
150.0	20.00	.7400	.8061	-.6611E-01
150.0	20.00	.7500	.8061	-.5611E-01
150.0	30.00	.7100	.7544	-.4444E-01
150.0	30.00	.7300	.7544	-.2444E-01
180.0	10.00	.8300	.8163	.1366E-01
180.0	10.00	.7800	.8163	.3634E-01
180.0	20.00	.8000	.7665	.3345E-01
180.0	20.00	.8000	.7665	.3345E-01
180.0	20.00	.8400	.7665	.7345E-01
180.0	30.00	.6400	.7080	-.6797E-01
180.0	30.00	.6400	.7080	-.6797E-01
180.0	30.00	.7400	.7080	.3203E-01
210.0	10.00	.8000	.7845	.1554E-01
210.0	10.00	.8400	.7845	.5554E-01
210.0	10.00	.7200	.7845	.6446E-01
210.0	20.00	.7700	.7289	.4107E-01
210.0	20.00	.7200	.7289	-.8925E-02
210.0	20.00	.7400	.7289	.1107E-01
210.0	30.00	.6700	.6644	.5643E-02
210.0	30.00	.7100	.6644	.4564E-01
210.0	30.00	.6400	.6644	-.2436E-01
240.0	10.00	.7600	.7538	.6179E-02
240.0	10.00	.7800	.7538	.2618E-01
240.0	10.00	.7800	.7538	.2618E-01
240.0	20.00	.7400	.6931	.4685E-01
240.0	20.00	.7300	.6931	.3685E-01
240.0	20.00	.8300	.6931	.1369
240.0	30.00	.7900	.6234	.1666
240.0	30.00	.7000	.6234	.7657E-01
240.0	30.00	.7400	.6234	.1166

The objective function value is .400225E+00

The number of function calls is : 62

The number of eigenvalue calculations is 7

The linear theory covariance matrix is :

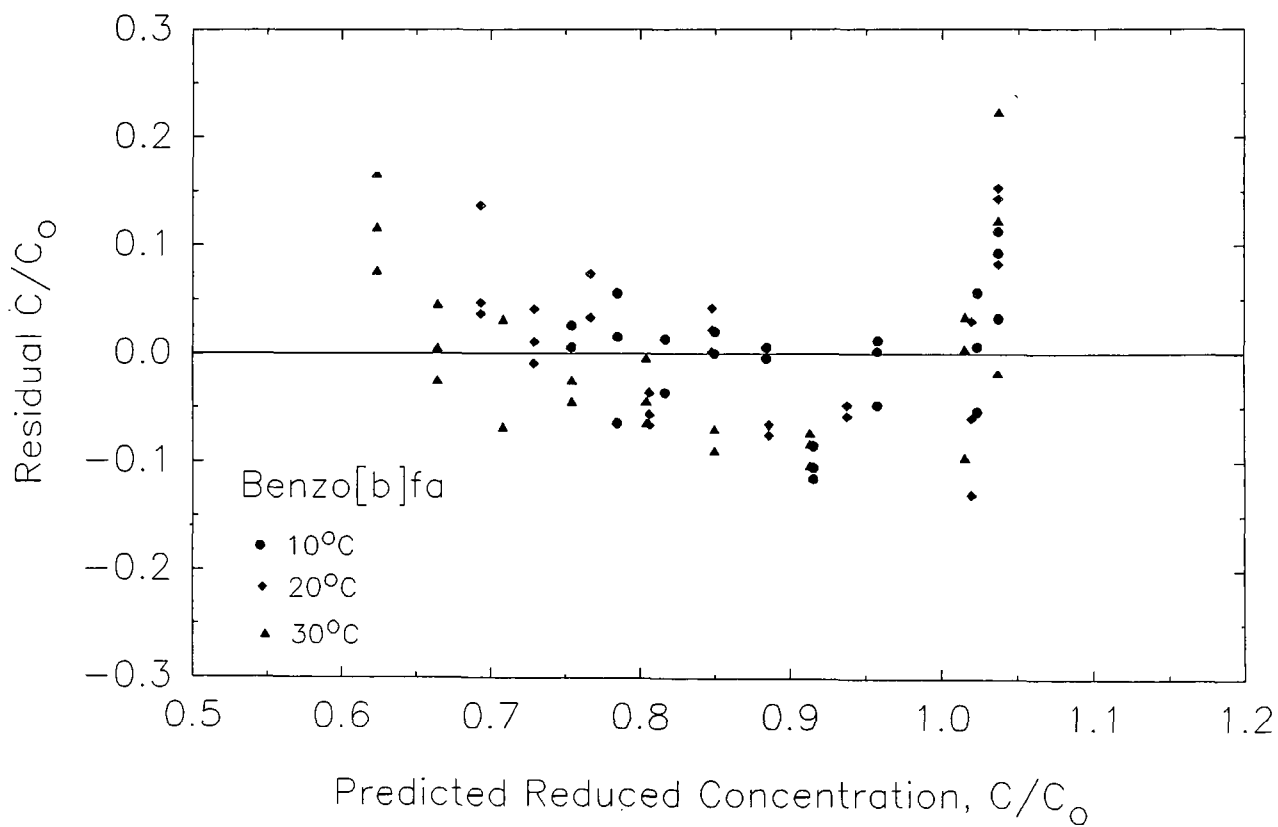
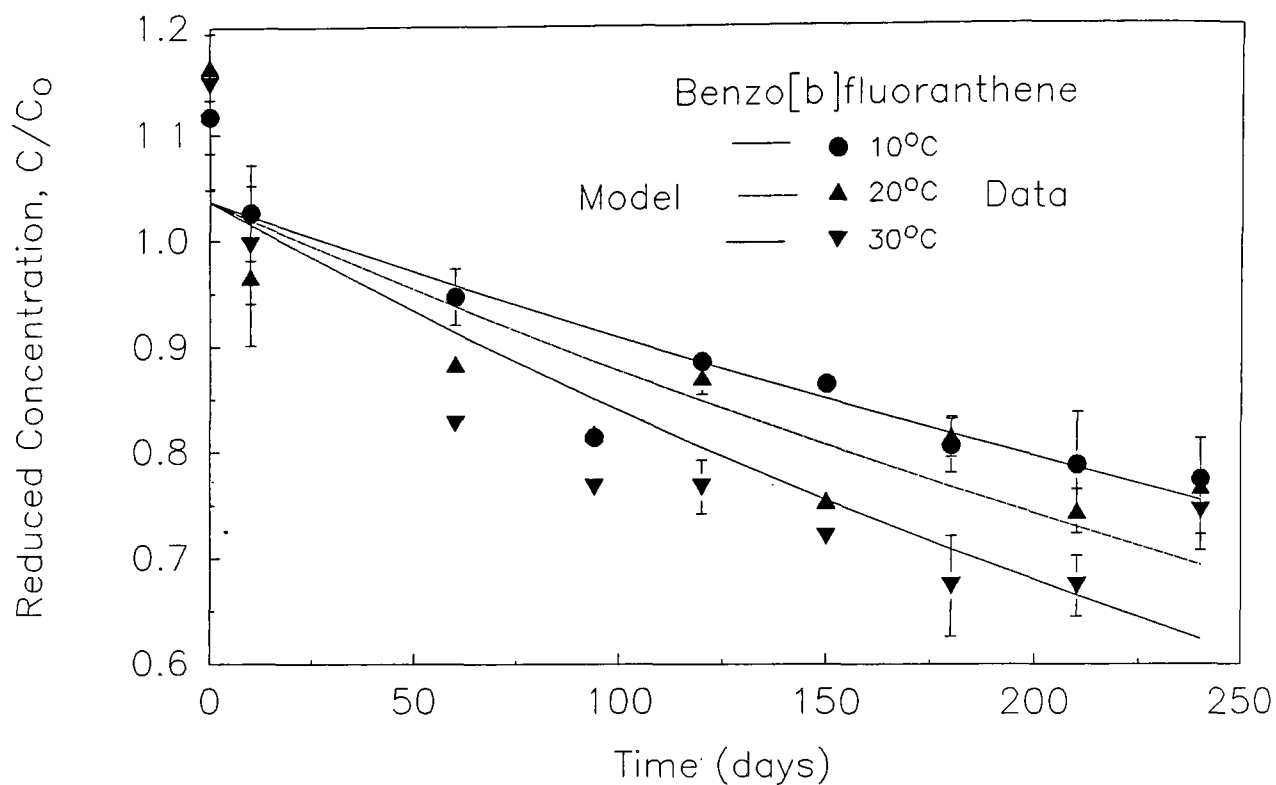
.143E-07		
.138E-05	.228E-03	
-.229E-06	-.178E-04	.350E-04

The linear theory correlation matrix is :

1.000		
.7647	1.000	
-.3229	-.1988	1.000

95% Confidence Intervals for the Parameters are :

	No.	Lower	Theta	Upper		
k_{20}	1	.14385E-02	<	.16776E-02	<	.19166E-02 day ⁻¹
C_o	2	1.0066	<	1.0368	<	1.0669
θ	3	1.0118	<	1.0236	<	1.0355



Non-Linear Least Squares Parameter Estimation

Chrysene Temperature Data

After 2 iteration(s), converged parameter estimates are

k_{20}	C_0	θ
.589910E-03 day ⁻¹	.100580E+01	.100295E+01

X(1) Time	X(2) Temp.	OBS C/C ₀	ETA Predicted	Resid
.0000	10.00	.9900	1.006	-.1580E-01
.0000	10.00	.9700	1.006	-.3580E-01
.0000	10.00	.9600	1.006	.4580E-01
.0000	20.00	.9700	1.006	-.3580E-01
.0000	20.00	.9700	1.006	-.3580E-01
.0000	20.00	1.010	1.006	.4202E-02
.0000	30.00	1.070	1.006	.6420E-01
.0000	30.00	1.040	1.006	.3420E-01
.0000	30.00	.9600	1.006	-.4580E-01
10.00	10.00	.9700	1.000	-.3005E-01
10.00	10.00	.9700	1.000	-.3005E-01
10.00	10.00	.9500	1.000	-.5005E-01
10.00	20.00	1.010	.9999	.1012E-01
10.00	20.00	.9600	.9999	.3988E-01
10.00	20.00	1.010	.9999	.1012E-01
10.00	30.00	1.030	.9997	.3029E-01
10.00	30.00	1.080	.9997	.8029E-01
10.00	30.00	1.000	.9997	.2939E-03
60.00	10.00	.9900	.9718	.1818E-01
60.00	10.00	1.000	.9718	.2818E-01
60.00	10.00	.9900	.9718	.1818E-01
60.00	20.00	.9700	.9708	.8209E-03
60.00	20.00	1.000	.9708	.2918E-01
60.00	20.00	1.020	.9708	.4918E-01
60.00	30.00	.9800	.9698	.1021E-01
60.00	30.00	.9800	.9698	.1021E-01
60.00	30.00	.9800	.9698	.1021E-01
94.00	10.00	.9000	.9531	-.5307E-01
94.00	10.00	.9200	.9531	-.3307E-01
94.00	10.00	.9300	.9531	-.2307E-01
94.00	20.00	.9300	.9515	-.2154E-01
94.00	20.00	.9300	.9515	.2154E-01
94.00	20.00	.9600	.9515	.8457E-02
94.00	30.00	.9400	.9500	-.9968E-02
94.00	30.00	.9200	.9500	-.2997E-01
94.00	30.00	.9300	.9500	-.1997E-01
120.0	10.00	.9700	.9390	.3101E-01
120.0	10.00	.9900	.9390	.5101E-01
120.0	20.00	.9900	.9371	.5294E-01
120.0	20.00	1.000	.9371	.6294E-01
120.0	20.00	1.010	.9371	.7294E-01
120.0	30.00	.9400	.9351	.4919E-02
120.0	30.00	.9500	.9351	.1492E-01
120.0	30.00	.9800	.9351	.4492E-01
150.0	10.00	.9300	.9230	.7012E-02
150.0	10.00	.9400	.9230	.1701E-01
150.0	10.00	.9400	.9230	.1701E-01

150.0	20.00	.8900	.9206	-.3062E-01
150.0	20.00	.8700	.9206	-.5062E-01
150.0	20.00	.8900	.9206	-.3062E-01
150.0	30.00	.8300	.9182	-.8819E-01
150.0	30.00	.9200	.9182	.1808E-02
180.0	10.00	.9300	.9073	.2274E-01
180.0	10.00	.9000	.9073	-.7263E-02
180.0	20.00	.9700	.9045	.6553E-01
180.0	20.00	.9800	.9045	.7553E-01
180.0	20.00	.9500	.9045	.4553E-01
180.0	30.00	.8500	.9016	-.5161E-01
180.0	30.00	.8200	.9016	-.8161E-01
180.0	30.00	.9600	.9016	.5839E-01
210.0	10.00	.9100	.8918	.1819E-01
210.0	10.00	.9500	.8918	.5819E-01
210.0	10.00	.8200	.8918	-.7181E-01
210.0	20.00	.9300	.8886	.4139E-01
210.0	20.00	.8700	.8886	-.1861E-01
210.0	20.00	.9000	.8886	.1139E-01
210.0	30.00	.8500	.8853	-.3533E-01
210.0	30.00	.8500	.8853	-.3533E-01
210.0	30.00	.8400	.8853	.4533E-01
240.0	10.00	.8200	.8766	-.5661E-01
240.0	10.00	.8300	.8766	-.4661E-01
240.0	10.00	.8300	.8766	-.4661E-01
240.0	20.00	.8300	.8730	-.4302E-01
240.0	20.00	.8400	.8730	-.3302E-01
240.0	20.00	.9300	.8730	.5698E-01
240.0	30.00	.9900	.8693	.1207
240.0	30.00	.8600	.8693	-.9335E-02
240.0	30.00	.8600	.8693	-.9335E-02

The objective function value is .139167E+00

The number of function calls is : 34

The number of eigenvalue calculations is 4

The linear theory covariance matrix is :

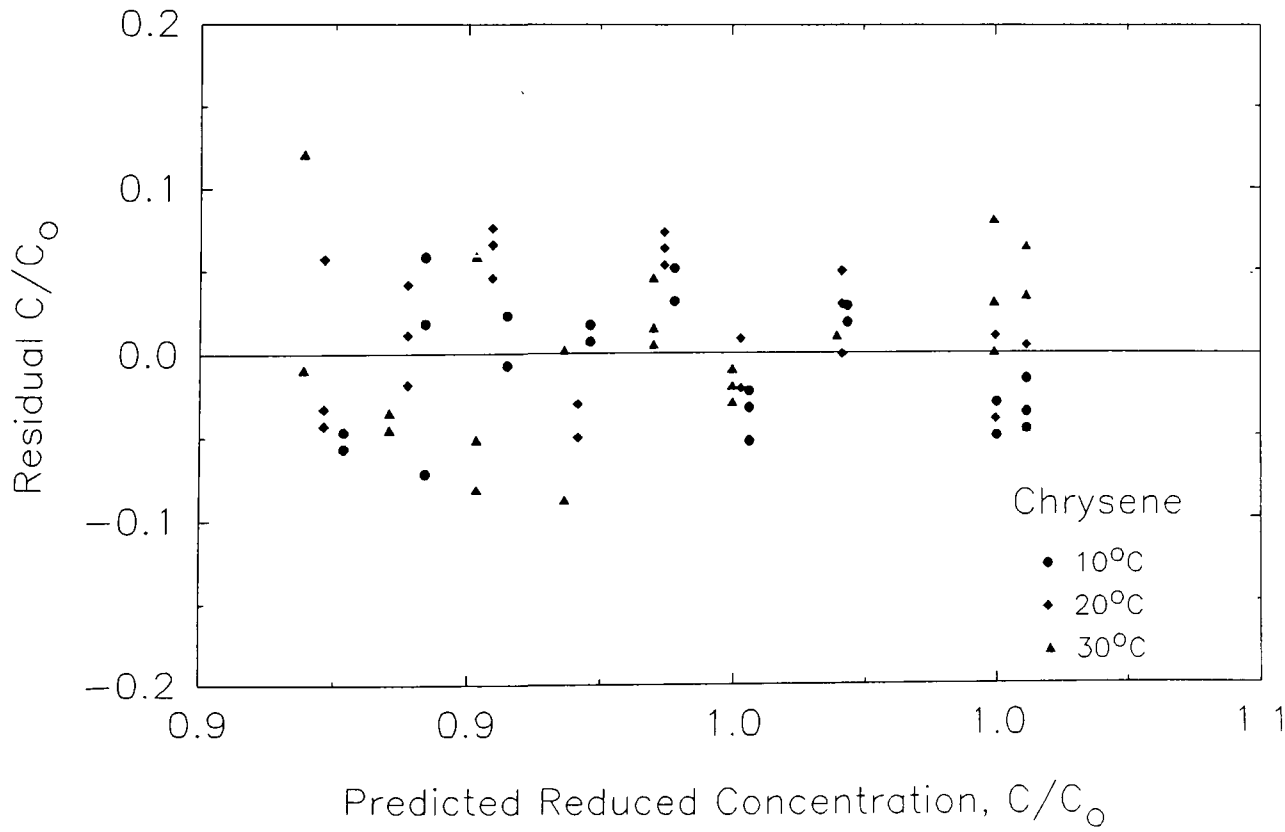
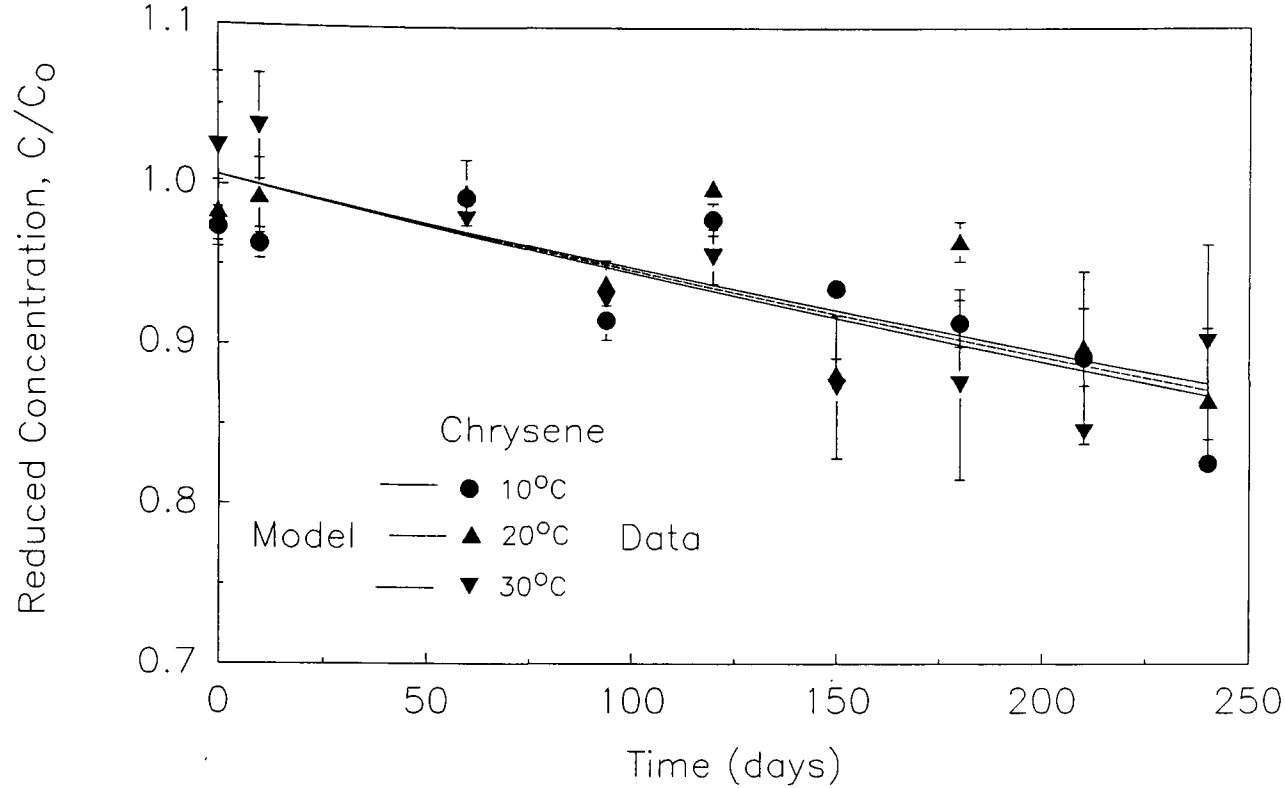
.393E-08		
.432E-06	.736E-04	
-.299E-07	-.201E-05	.621E-04

The linear theory correlation matrix is :

1.000		
.8027	1.000	
-.6049E-01	-.2971E-01	1.000

95% Confidence Intervals for the Parameters are :

	No.	Lower	Theta	Upper		
k_{20}	1	.46471E-03	<	.58991E-03	<	.71511E-03 day ⁻¹
C_o	2	.98868	<	1.0058	<	1.0229
θ	3	.98722	<	1.0029	<	1.0187



Non-Linear Least Squares Parameter Estimation

Fluorene Temperature Data

After 4 iteration(s), converged parameter estimates are

k_{20}		C_0	θ	
.155144E-01 day ⁻¹		.982529E+00	.107437E+01	
X(1) Time	X(2) Temp.	OBS C/C ₀	ETA Predicted	Resid
.0000	10.00	.9400	.9825	-.4253E-01
.0000	10.00	.9300	.9825	-.5253E-01
.0000	10.00	.9300	.9825	.5253E-01
.0000	20.00	.9400	.9825	.4253E-01
.0000	20.00	.9500	.9825	.3253E-01
.0000	20.00	.9700	.9825	-.1253E-01
.0000	30.00	1.000	.9825	.1747E-01
.0000	30.00	.9500	.9825	-.3253E-01
.0000	30.00	.8700	.9825	-.1125
10.00	10.00	.8700	.9109	-.4088E-01
10.00	10.00	.8900	.9109	-.2088E-01
10.00	10.00	.8600	.9109	-.5088E-01
10.00	20.00	.8600	.8413	.1867E-01
10.00	20.00	.8300	.8413	-.1133E-01
10.00	20.00	.8700	.8413	.2867E-01
10.00	30.00	.7400	.7150	.2502E-01
10.00	30.00	.7700	.7150	.5502E-01
10.00	30.00	.7000	.7150	-.1498E-01
60.00	10.00	.8200	.6238	.1962
60.00	10.00	.8200	.6238	.1962
60.00	10.00	.8200	.6238	.1962
60.00	20.00	.2300	.3873	-.1573
60.00	20.00	.2500	.3873	.1373
60.00	20.00	.2800	.3873	-.1073
60.00	30.00	.1700	.1459	.2411E-01
60.00	30.00	.1700	.1459	.2411E-01
94.00	10.00	.7400	.4822	.2578
94.00	10.00	.7600	.4822	.2778
94.00	10.00	.7600	.4822	.2778
94.00	20.00	.1700	.2286	.5855E-01
94.00	20.00	.2000	.2286	.2855E-01
94.00	20.00	.2300	.2286	.1445E-02
94.00	30.00	.1200	.4951E-01	.7049E-01
94.00	30.00	.1300	.4951E-01	.8049E-01
94.00	30.00	.9000E-01	.4951E-01	.4049E-01
120.0	10.00	.7100	.3960	.3140
120.0	10.00	.3400	.3960	-.5603E-01
120.0	20.00	.1900	.1527	.3731E-01
120.0	20.00	.1800	.1527	.2731E-01
120.0	20.00	.2400	.1527	.8731E-01
120.0	30.00	.1200	.2166E-01	.9834E-01
120.0	30.00	.1100	.2166E-01	.8834E-01
120.0	30.00	.9000E-01	.2166E-01	.6834E-01
150.0	10.00	.1600	.3156	-.1556
150.0	10.00	.1700	.3156	-.1456
150.0	10.00	.1200	.3156	-.1956
150.0	20.00	.5000E-01	.9587E-01	-.4587E-01

150.0	20.00	.6000E-01	.9587E-01	-.3587E-01
150.0	20.00	.7000E-01	.9587E-01	-.2587E-01
150.0	30.00	.1000E-01	.8347E-02	.1653E-02
150.0	30.00	.1000E-01	.8347E-02	.1653E-02
180.0	10.00	.8000E-01	.2514	-.1714
180.0	10.00	.9000E-01	.2514	-.1614
180.0	20.00	.5000E-01	.6019E-01	-.1019E-01
180.0	20.00	.5000E-01	.6019E-01	-.1019E-01
180.0	20.00	.2000E-01	.6019E-01	.4019E-01
180.0	30.00	.2000E-01	.3217E-02	.1678E-01
180.0	30.00	.2000E-01	.3217E-02	.1678E-01
180.0	30.00	.2000E-01	.3217E-02	.1678E-01
210.0	10.00	.1000	.2003	-.1003
210.0	10.00	.1400	.2003	-.6034E-01
210.0	10.00	.8000E-01	.2003	-.1203
210.0	20.00	.4000E-01	.3779E-01	.2208E-02
210.0	20.00	.4000E-01	.3779E-01	.2208E-02
210.0	20.00	.4000E-01	.3779E-01	.2208E-02
210.0	30.00	.2000E-01	.1239E-02	.1876E-01
210.0	30.00	.1000E-01	.1239E-02	.8761E-02
210.0	30.00	.1000E-01	.1239E-02	.8761E-02
240.0	10.00	.8000E-01	.1596	-.7963E-01
240.0	10.00	.7000E-01	.1596	-.8963E-01
240.0	10.00	.8000E-01	.1596	.7963E-01
240.0	20.00	.3000E-01	.2373E-01	.6272E-02
240.0	20.00	.4000E-01	.2373E-01	.1627E-01
240.0	20.00	.3000E-01	.2373E-01	.6272E-02
240.0	30.00	.2000E-01	.4776E-03	.1952E-01

The objective function value is .773754E+00

The number of function calls is : 53

The number of eigenvalue calculations is 6

The linear theory covariance matrix is :

.118E-05		
.130E-04	.731E-03	
.447E-05	.332E-05	.699E-04

The linear theory correlation matrix is :

1.000		
.4422	1.000	
.4924	.1467E-01	1.000

95% Confidence Intervals for the Parameters are :

	No.	Lower	Theta	Upper	
k_{20}	1	.13350E-01 <	.15514E-01 <	.17679E-01	day ⁻¹
C_o	2	.92856 <	.98253 <	1.0365	
θ	3	1.0577 <	1.0744 <	1.0911	

